Phase II: Correlation Between Experimental and Finite Element Analysis Alaska Bridge 255- Chulitna River Bridge

FINAL PROJECT REPORT

by

J. Leroy Hulsey, Ph.D., P.E., S.E
Feng Xioa, Graduate Student
University of Alaska Fairbanks

J.Daniel Dolan, Ph.D., P.E.
Washington State Unversity

for

Pacific Northwest Transportation Consortium (PacTrans)
USDOT University Transportation Center for Federal Region 10
University of Washington
More Hall 112, Box 352700
Seattle, WA 98195-2700

Alaska Department of Transportation & Public Facilities

Alaska University Transportation Center

Phase II: Correlation Between Experimental and Finite Element Analysis

Alaska Bridge 255– Chulitna River Bridge

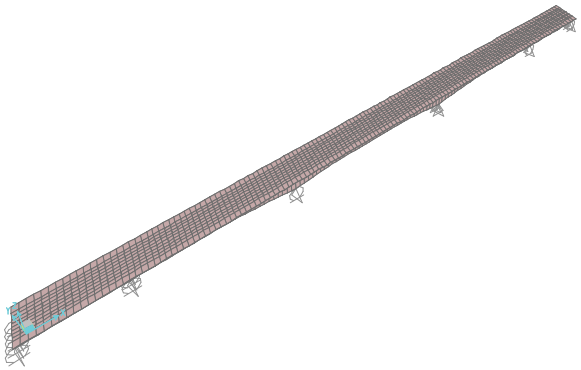

J. Leroy Hulsey, Ph.D., P.E., S.E.
Professor of Civil & Environmental Engineering
University of Alaska Fairbanks

Feng Xiao, Graduate Student
University of Alaska Fairabanks

J. Daniel Dolan, Ph.D., P.E.
Department of Civil & Environmental Engineering
Washington State University

March 2014

Alaska University Transportation Center
Duckering Building Room 245
P.O. Box 755900
Fairbanks, AK 99775-5900

Alaska Department of Transportation
Research, Development, and Technology Transfer
2301 Peger Road
Fairbanks, AK 99709-5399

INE/ AUTC 14.04

Technical Report Documentation Page

1. Report No.	2. Government Accession No.	3. Recipient's Catalog No.
2012-S-UAF-0013	01538100	

4. Title and Subtitle
Phase II: Correlation Between Experimental and Finite Element Analysis
Alaska Bridge 255- Chulitna River Bridge

5. Report Date
September 15, 2014

6. Performing Organization Code

7. Author(s)
J. Leroy Hulsey, Feng Xioa, J.Daniel Dolan

8. Performing Organization Report No.
13-739439

9. Performing Organization Name and Address

PacTrans
Pacific Northwest Transportation Consortium, University Transportation Center for Region 10
University of Washington More Hall 112
Seattle, WA 98195-2700

Civil and Environmental Engineering Department
University of Alaska Fairbanks, P.O. Box 755900, Fairbanks, AK 99775-5900

10. Work Unit No. (TRAIS)

11. Contract or Grant No.
DTRT12-UTC10

12. Sponsoring Organization Name and Address
United States of America
Department of Transportation
Research and Innovative Technology Administration

13. Type of Report and Period Covered
Research 9/1/2012-7/31/2014

14. Sponsoring Agency Code

15. Supplementary Notes
Report uploaded at www.pacTrans.org

16. Abstract

In this study, we will monitor the behavior of the Alaska Chulitna Bridge for the specific purpose of assisting the DOT in performing an accurate condition assessment of this bridge.

Based on the state-of-the-art SHM knowledge and technologies with a specific interest in those which could be used on bridges in cold, remote regions, the objective of this study is to provide important information for structural condition assessment of the Chulitna River Bridge.

Proposed SHM objectives are listed below—applicable to all bridges:

Develop a SHM protocol including preferred system integrator, software, instrumentation, and sensors suitable for Alaska's remote, harsh weather locations.
Develop criteria to incorporate SHM into the state's bridge management process.

The established SHM system for ADOT&PF will be able to monitor performance of bridges subjected to extreme temperature and conditions—an aspect that is very important information for assessment of the structural condition and potential remaining service life of Alaska bridges.

17. Key Words	18. Distribution Statement
Condition assessment, SHM, Final Element Model, Inventory Load Rating	No restrictions.

19. Security Classification (of this report)	20. Security Classification (of this page)	21. No. of Pages	22. Price
Unclassified.	Unclassified.		NA

Form DOT F 1700.7 (8-72) **Reproduction of completed page authorized**

Disclaimer

The contents of this report reflect the views of the authors, who are responsible for the facts and the accuracy of the information presented herein. This document is disseminated under the sponsorship of the U.S. Department of Transportation's University Transportation Centers Program, in the interest of information exchange. The Pacific Northwest Transportation Consortium and the U.S. Government assumes no liability for the contents or use thereof.

Notice

This document is disseminated under the sponsorship of the U.S. Department of Transportation in the interest of information exchange. The U.S. Government assumes no liability for the use of the information contained in this document.

The U.S. Government does not endorse products or manufacturers. Trademarks or manufacturers' names appear in this report only because they are considered essential to the objective of the document.

Quality Assurance Statement

The Federal Highway Administration (FHWA) provides high-quality information to serve Government, industry, and the public in a manner that promotes public understanding. Standards and policies are used to ensure and maximize the quality, objectivity, utility, and integrity of its information. FHWA periodically reviews quality issues and adjusts its programs and processes to ensure continuous quality improvement.

Author's Disclaimer

Opinions and conclusions expressed or implied in the report are those of the author. They are not necessarily those of the Alaska DOT&PF or funding agencies.

SI* (MODERN METRIC) CONVERSION FACTORS

APPROXIMATE CONVERSIONS TO SI UNITS

Symbol	When You Know	Multiply By	To Find	Symbol
		LENGTH		
in	inches	25.4	millimeters	mm
ft	feet	0.305	meters	m
yd	yards	0.914	meters	m
mi	miles	1.61	kilometers	km
		AREA		
in^2	square inches	645.2	square millimeters	mm^2
ft^2	square feet	0.093	square meters	m^2
yd^2	square yard	0.836	square meters	m^2
ac	acres	0.405	hectares	ha
mi^2	square miles	2.59	square kilometers	km^2
		VOLUME		
fl oz	fluid ounces	29.57	milliliters	mL
gal	gallons	3.785	liters	L
ft^3	cubic feet	0.028	cubic meters	m^3
yd^3	cubic yards	0.765	cubic meters	m^3
		NOTE: volumes greater than 1000 L shall be shown in m^3		
		MASS		
oz	ounces	28.35	grams	g
lb	pounds	0.454	kilograms	kg
T	short tons (2000 lb)	0.907	megagrams (or "metric ton")	Mg (or "t")
		TEMPERATURE (exact degrees)		
^oF	Fahrenheit	5 (F-32)/9 or (F-32)/1.8	Celsius	^oC
		ILLUMINATION		
fc	foot-candles	10.76	lux	lx
fl	foot-Lamberts	3.426	$candela/m^2$	cd/m^2
		FORCE and PRESSURE or STRESS		
lbf	poundforce	4.45	newtons	N
lbf/in^2	poundforce per square inch	6.89	kilopascals	kPa

APPROXIMATE CONVERSIONS FROM SI UNITS

Symbol	When You Know	Multiply By	To Find	Symbol
		LENGTH		
mm	millimeters	0.039	inches	in
m	meters	3.28	feet	ft
m	meters	1.09	yards	yd
km	kilometers	0.621	miles	mi
		AREA		
mm^2	square millimeters	0.0016	square inches	in^2
m^2	square meters	10.764	square feet	ft^2
m^2	square meters	1.195	square yards	yd^2
ha	hectares	2.47	acres	ac
km^2	square kilometers	0.386	square miles	mi^2
		VOLUME		
mL	milliliters	0.034	fluid ounces	fl oz
L	liters	0.264	gallons	gal
m^3	cubic meters	35.314	cubic feet	ft^3
m^3	cubic meters	1.307	cubic yards	yd^3
		MASS		
g	grams	0.035	ounces	oz
kg	kilograms	2.202	pounds	lb
Mg (or "t")	megagrams (or "metric ton")	1.103	short tons (2000 lb)	T
		TEMPERATURE (exact degrees)		
^oC	Celsius	1.8C+32	Fahrenheit	^oF
		ILLUMINATION		
lx	lux	0.0929	foot-candles	fc
cd/m^2	$candela/m^2$	0.2919	foot-Lamberts	fl
		FORCE and PRESSURE or STRESS		
N	newtons	0.225	poundforce	lbf
kPa	kilopascals	0.145	poundforce per square inch	lbf/in^2

*SI is the symbol for the International System of Units. Appropriate rounding should be made to comply with Section 4 of ASTM E380.
(Revised March 2003)

Table of Contents

List of Figures

List of Tables

Disclaimer

The contents of this report reflect the views of the authors, who are responsible for the facts and the accuracy of the information presented herein. This document is disseminated under the sponsorship of the U.S. Department of Transportation's University Transportation Centers Program, in the interest of information exchange. The Pacific Northwest Transportation Consortium and the U.S. Government assume no liability for the contents or use thereof.

Executive Summary

This report provides the outcomes from Phase 2 of a study that used a structural health monitoring system (SHMS) to evaluate the Chulitna River Bridge on the Parks Highway. This bridge is 790 feet long, 42 foot 2 inches wide and has 5 spans.

Phase 1 (SHMS): In spring/summer 2012, the Alaska University Transportation Center (AUTC) research team in collaboration with the Alaska Department of Transportation and Public Facilities selected a SHMS for possible use on the Chulitna River Bridge. The remaining summer months were spent training, selecting sensors, and placing instrumentation on the bridge. In a joint effort, the instrumentation was placed by AUTC and CMS (the SHMS contractor in Lawensburg, Georgia). Prior to completing installation of the instrumentation, the bridge's response to excitation was monitored with 15 accelerometers along the bridge centerline. The frequency response data provided a bridge-condition baseline for the work conducted in September 2012. On September 9, 2012, the research team prepared to load test the bridge. Two belly dump trucks and one side dump truck belonging to ADOT&PF were measured, loaded with sand, and weighed. Prior to testing, CMS calibrated the sensors, and AUTC prepared the test procedure. On September 10, 2012, we subjected the bridge to 17 different static and dynamic load combinations using the three dump trucks (2 bellies and 1 side dump). That effort ended Phase 1.

Phase 2 (Bridge Evaluation): During Phase 2, we tested, modified, and calibrated a SAP 2000 three-dimensional finite element model (FEM) to correlate with the test data obtained through the SHMS and the ambient vibration data for the structure. The SHMS data are referred to as *local* experimental data. Local data are strains, displacements, etc., at discrete points on the

bridge, and the values are recorded by the SHMS. The ambient vibration test data are referred to as *global* data. That is, vibration response is influenced by stiffness and mass, which has a "smearing affect" and does not represent behavior at a point.

The model was calibrated to September 12, 2012, SHMS local static and dynamic test data resulting from the three loaded ADOT&PF dump trucks. The model was also calibrated to the global ambient vibration digital test data taken in August 2012 and again in May 2013 during an ADOT&PF bridge inspection. Global data were recorded using a portable data acquisition system to collect dynamic data. The test equipment consisted of three parts: portable uniaxial accelerometers, an integrator, and a laptop and cables. The portable accelerometer is an EpiSensor force balance accelerometer ES-U2. The EpiSensor has user-selectable full-scale recording ranges of ±4g, ±2g, ±1g, ±1/2g, or ±1/4g. Its bandwidth is from DC to 200 Hz. In weak motion, the weight of the instrument and friction between the feet and deck ensure accurate reproduction of ground motion. Each accelerometer requires zero adjusting, and each is calibrated on-site. Fifteen accelerometers were put on the surface of the concrete bridge to record the global frequency response data.

Outcomes: We provide three outcomes in this study. The first is a calibrated FEM that accurately simulates the response of the Chulitna River Bridge under a given set of loads. The second outcome provides an inventory load rating for the bridge, and the third outcome provides the live load states of stress for AASHTO traffic loads.

Outcome 1 – Finite Element Model

- We have a finite element model that is now calibrated against two different data sets, measured ambient frequencies (global data for 2012 and 2013), and SHMS (local strain for September 10, 2012) data. The results are satisfactory, and the program can

be used reliably to evaluate bridge response such as HL-93 AASHTO loads and special permit loads that will be traveling across the bridge.

Outcome 2 – Inventory Load Rating

We conducted an inventory load rating of the bridge for the following conditions:

- As-is (bridge is not supported at five rocker bearing supports):
  - Two lanes loaded using an operating LRFR HL-93 loading
  - Three lanes loaded using an operating LRFR HL-93 loading
  - One lane, special permitted load (truck drives down the centerline)
- Modified Bridge: Consider that filler plates are installed under the five bearing supports that are separated from the structure. This change ensures that the superstructure is in contact with the rocker bearings (all supports are functioning properly).

Between one and four members making up the interior truss girder near the bearing supports did not meet the inventory rating requirements. In three of the four members, the dead load stresses were around 50% of the capacity of these members. Induced dead load stresses that resulted from the bridge widening are not known; this depends on how work occurred in 1993.

CHAPTER 1.0 INTRODUCTION

History: Bridges in Alaska can be subjected to extremely cold temperatures and, depending on location, can be subjected to excessively deep snow, strong winds, and or significant earthquake activity. Moreover, bridges in Alaska are often located in remote areas, and because of the harsh environment, maintenance and rehabilitation can be very expensive.

Asset management costs for maintenance, rehabilitation, and replacement depend on reliable inspection and condition assessment. Compared with other states, bridge monitoring in Alaska can provide a cost savings and can be a valuable tool in evaluating structural condition. However, power and or phone service is not always available at a remote site, and this may be a challenge for real-time data retrieval.

In spring 2012, the ADOT&PF selected the Chulitna River Bridge for study to determine if a structural health monitoring system (SHMS) was appropriate for evaluating the state's bridges and if SHMS data would be reliable and of value to the department. The bridge is located at Milepost 132.7 on the Parks Highway between Fairbanks and Anchorage, Alaska. This highway is the most direct route connecting Anchorage to Fairbanks and the oil fields in Prudhoe Bay. Because of oil field operational demands, overloaded vehicles up to 410,000 pounds travel over this bridge regularly. In 2004, ADOT&PF discovered five locations where the bridge superstructure did not sit on its support bearings. Some unusual features of this bridge and the fact that it is not supported as designed make it a likely candidate for evaluation.

Bridge Details: The Chulitna River Bridge was built in 1970 on a 22-degree skew. It is 790-feet long with five spans of 100, 185, 220, 185, and 100 feet. The superstructure was a 34-foot-wide by 6¾-inch-thick cast-in-place concrete deck supported by two exterior continuous longitudinal variable depth girders and three interior stringers. The girder stringers are spaced at

7 feet on center. The interior stringers are supported by a cross frame that is carried by the exterior girders. The cross frame was detailed to transfer dead loads and traffic loads to the exterior girders. Interior stringers were W21x44, and the exterior girders had a variable depth web that varied from 84 inches deep in the first and fifth spans to 108 inches deep in the middle spans. At Piers 2 and 4, the exterior girder web has a haunch depth of 148 inches. At Pier 3, the exterior girder web has a haunch depth of 168 inches.

In 1993, the bridge deck was widened from a 34-foot cast-in-place concrete deck to a 42-foot 2-inch concrete deck made of precast concrete deck panels. The increased load was accounted for by strengthening the variable depth exterior girders and converting the W21x44 interior stringers to an interior truss girder; the W21x44 became the upper chord of the truss (Fig. 1.1).

Figure 1.1 Current picture of the Chulitna River Bridge

In September 2010, Bridge Diagnostics, Inc. (BDI) load tested the bridge. The primary goal of this test was to evaluate how the load is distributed from the top of the driving surface into the support girders and the corresponding cross frames. The test results were compared with

an HDR finite element model (FEM). Some of the unique features of this bridge are (a) the interior truss girders are substantially different from the two exterior girders, and (b) five rocker bearings are either not in contact with the masonry plates or in partial contact with the masonry plates. The bearing locations include all three truss bearings at Pier 3 and the two lane truss bearings at Pier 5 (Fig. 1.2).

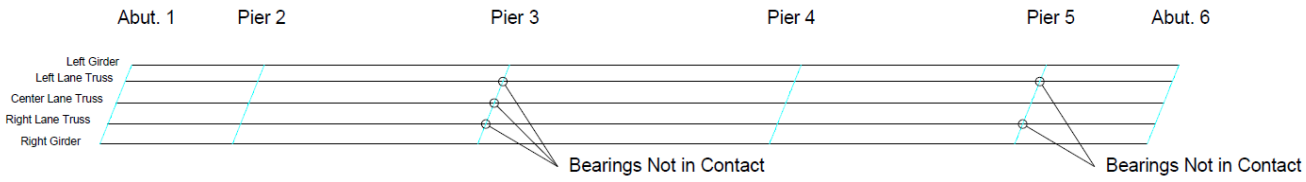

Figure 1.2 Plan view: Bearings that are not contact with masonry plates

The ADOT&PF and AUTC jointly funded a research grant to UAF in spring 2012 to develop a SHMS that could be used to monitor Alaska bridges, instrument the bridge, calibrate the system, and load test the structure. This research effort was Phase 1, to be completed at or around the end of September 2012.

After September 2012, a second phase of research to study this bridge began. In Phase 2, ADOT&PF, AUTC, and PacTrans funded UAF and Washington State University (WSU) to monitor the bridge through December 31, 2013. In addition to monitoring the bridge response to traffic, the research team was to develop and calibrate a FEM that would provide a reliable bridge behavioral response to traffic AASHTO loading and special permitted vehicles. This document is the Phase 2 report. The report provides a summary of experimental data obtained from two different field-evaluation systems: local and global. For the purpose of this report, the local system provides response data at localized locations on the bridge. Localized strains, temperatures, etc., are obtained using the SHMS.

Localized response data are obtained through the use fiber-optic sensors such as strain gauges, tilt meters, and temperature sensors at specific locations established through the previous Phase 1 study. In an attempt to understand and evaluate the response of the Chulitna River Bridge to traffic loads, the Phase 1 research team in collaboration with ADOT&PF selected and installed 73 sensors and introduced a global field monitoring system. This methodology is an ambient acceleration study that attempts to identify natural frequencies of the structure once it is excited. Horizontal, vertical, and transverse frequencies were measured by 15 portable accelerometers distributed across the top deck of the structure. In this report, these frequency responses are identified as global data.

Phase 1: The Chulitna River Bridge was instrumented at the end of August 2012 through September 9, 2012. While instrumentation was being installed on the bridge, the research team conducted “ambient frequency tests” using 15 portable accelerometers. This testing was not part of the research plan, but the research team believed that because it is fast and the frequencies provide a baseline for the health of the structure, the test can be an important methodology for evaluating the overall structural condition. This type of testing is inexpensive and can be an important tool if used during bridge inspection.

Structural health monitoring can be used to provide early warnings about bridge safety and to monitor structural condition and changes in condition in real time (by monitoring strain, acceleration, displacement, temperature, etc). Other uses include providing valuable data for engineers who are preparing asset management plans.

Phase 2: In this report, we illustrate that we have a FEM that is now calibrated against two different data sets: measured ambient frequencies (global data) and SHM (local strain data).

The results are satisfactory and can be used as a tool to evaluate the behavior of the bridge for a given traffic condition.

The mid-span loading report on the Chulitna River Bridge (Hulsey and Xiao 2013) and previous ambient test research (Xiao et al. 2012) indicate that large errors exist in the HDR, Inc. FEM. Table 1.1 shows the errors between measured and calculated frequencies. These values were based on the HDR FEM prior to modification. Tables 1.2 and 1.3 provide a correlation between experimental sensor response and calculated values using the HDR FEM prior to modification (Hulsey and Xiao 2013; Xiao et al. 2012).

According to Tables 1.1, 1.2, and 1.3, the largest error between the measured global frequency data and calculated data is -10.2%. The largest error between measured local strain data and calculated data is 512% (see Table 5.2). To enhance the predictability of the results provided by the FEM for both global and local values, the HDR FEM required modification.

Table 1.1 Natural frequencies prior to modifying the HDR FEM

Mode	Field Measurement (Hz)	HDR FE Data (Hz)	Difference (%)
Longitudinal Mode 1	1.500	1.584	-5.6
Longitudinal Mode 2	2.190	2.389	-9.1
Vertical Mode 1	2.846	3.135	-10.2
Vertical Mode 2	3.224	3.390	-5.1
Vertical Mode 3	4.586	4.757	-3.7
Transverse Mode 1	2.095	2.262	-8.0
Transverse Mode 2	2.346	2.504	-6.7
Transverse Mode 3	2.782	2.847	-2.3

Table 1.2 Strain differences at the mid-span flange for Span 3 before model modifications (%)

Load Case	Location	1	2	3	4	5
	Sensor Number	R3	C9	C12	C15	L3
Top Flange	Field Measurement	-42.1	32.6	21.2	23.6	-59.3
	HDR FE Data					
Bottom Flange	Field Measurement	9.8	65.2	50.7	49.4	8.0
	HDR FE Data					

Table 1.3 Stress difference at the middle of Span 3 for the lower chord before model modifications (%)

Load Case	Location	1	2	3
	Sensor Number	R3	C9	C12
Top Flange	Field Measurement	-51.5	-53.6	-66.4
	HDR FE Data			

The FEM was modified by starting with HDR's version. Eighteen variables were selected for study: 4 girder flanges, 6 stringer flanges, 3 lower chords on the composite trusses, the elastic modulus for the concrete deck, the cross frame geometry, and 3 spring supports. These variables were selected to identify the (a) structural sensitivity, (b) load paths, and (c) stiffness contributions of the deck. Improvements were evaluated by using an objective function. This function is the error between field measurement data and calculated FEM results. The objective function was divided into two categories: global values and local values. Where applicable, objective functions were further subdivided for study. For example, a global-level objective function was used to evaluate the errors between measured frequencies and the FEM calculated frequencies in three different directions. The local-level objective functions are the errors between measured and FEM-calculated strain values. In Phase I, sensors were installed on the flanges of the longitudinal members at the middle of Span 2, 3 and 4 (girder and stringer flange,

and the lower chord of the composite truss) (Hulsey et al. 2012a). These sensor data were used to check the bridge's longitudinal behavior. Sensor data located on the diagonals (cross frames at Pier 3 and Pier 5) and roller bearings at Piers 3 and 5 were used to evaluate the bridge's transverse behavior.

The following chapters illustrate the methodology used to modify and improve the FEM so that it is now a reliable tool for use in evaluating bridge response when subjected to traffic loads, heavy trucks, permitted loads, climate, earthquake, river flow and debris that builds up against the piers.

CHAPTER 2.0 SIMPLE ACCURACY TEST

Before model changes were made, simple accuracy tests were performed on HDR's bridge model. That is, the number of elements (original mesh) was increased in an effort to evaluate the results for a newly refined mesh. This test was conducted to ensure that it would converge to provide a reasonable estimate of the structural response. The desired level of accuracy was set at 2%. Subsequently, the mesh size was reduced to half its current size to determine if the resulting displacements and forces would change significantly or if the change was small enough to be considered acceptable. Multiple locations on the bridge were checked. These locations were ones of critical interest to the project (i.e., high tension, large displacement, etc.). Nine sections were considered when checking the strains and stresses. These nine sections are located in different spans and sides of the bridge. Four longitudinal displacements on different sides of the abutments were selected for checking. We refined the mesh for the FEM to half its current size in both lines and areas. In Table 2.1, the error shows the difference between the original HDR model and the refined model. This comparison is based on three trucks that were stopped and positioned so that the front axles were 369 feet from the south abutment (Abutment 1); the three trucks were in the middle of Span 3.

The locations that are presented in Table 2.1 are illustrated in Figure 2.1. Table 2.1 indicates that the error between the two models is low. Ignoring the sign, the largest error is 1.04%, which is within the acceptable the level of accuracy. In general, the fine mesh used in the HDR model should give sufficiently accurate results.

Table 2.1 Simple accuracy comparison between the HDR model and the refined model

	Locations		Number	HDR Model	Refined Model	Error (%)
Force (lbs)	Mid-Span 2 Lower Chord	Downstream Side	1	-25,388	-25,476	-0.35
		Middle	2	-25,739	-25,858	-0.46
		Upstream Side	3	-26,612	-26,673	-0.23
	Mid-Span 3 Lower Chord	Downstream Side	4	80,867	81,199	-0.41
		Middle	5	83,554	83,893	-0.41
		Upstream Side	6	81,238	81,584	-0.43
	Mid-Span 4 Lower Chord	Downstream Side	7	-26,447	-26,562	-0.43
		Middle	8	-25,474	-25,624	-0.59
		Upstream Side	9	-25,546	-25,625	-0.31
Displacement Long. Dir. (mm)	Abutment 1 Roller Support	Downstream Side	10	-2.81	-2.84	-1.04
		Upstream Side	11	-2.82	-2.84	-0.66
	Abutment 2 Roller Support	Downstream Side	12	-2.21	-2.23	-0.92
		Upstream Side	13	-2.21	-2.21	-0.12

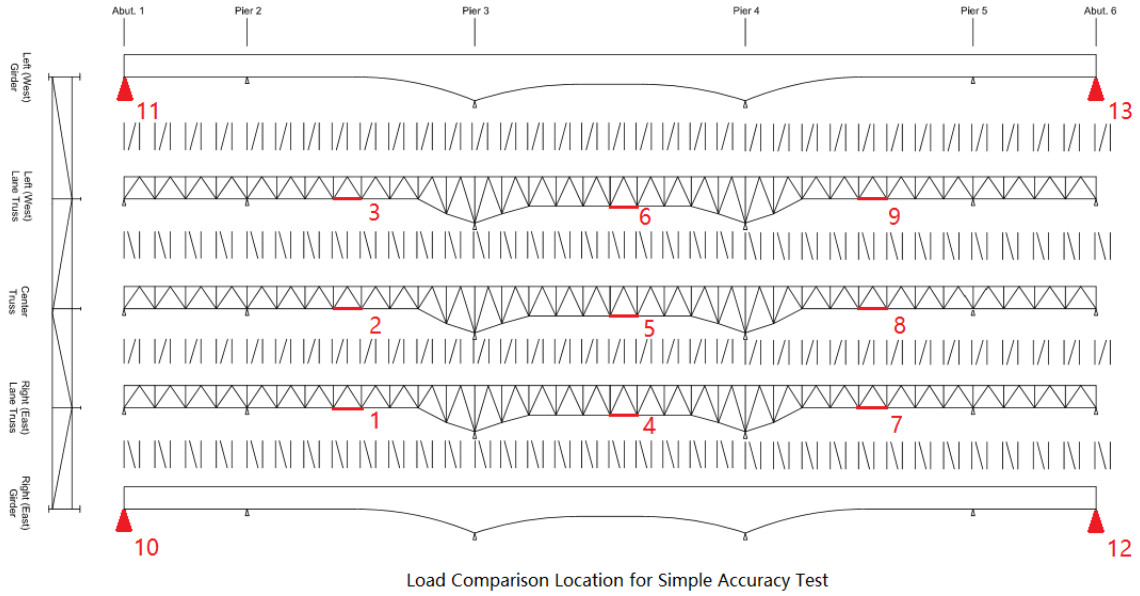

Figure 2.1 Locations where the influence of mesh refinement was checked (see Table 2.1).

At this point, the results of this test simply prove that if this model represents the actual bridge structure, the model will provide sufficiently accurate strains, displacements, and forces for a given set of loads. The results of this test do not prove that the model represents the bridge structure that is being studied.

CHAPTER 3.0 LONGITUDINAL BEHAVIOR TEST

Thirteen fiber-optic strain sensors were installed in Phase 1 at the middle of Span 3 (Hulsey et al. 2012a). The strains in these sensors were used to evaluate the influence of the three ADOT&PF trucks driving side by side (Hulsey et al. 2012b).

Figures 3.1, 3.2, and 3.3 show a comparison between stresses obtained from measured strain data and the "before modification" HDR FEM calculated mid-span stresses. The results indicate that the FEM-calculated stresses carried by the composite trusses are higher than measured; that is, calculated lower chord stresses are higher than measured (Hulsey and Xiao 2013). This finding illustrates that the FEM does not properly represent the distribution of stiffness between the bridge composite stringers and the girders. In consideration of these problems, 14 objective functions (variables) were selected for study. Modifications to the objective functions affected load distribution for the composite trusses and girders.

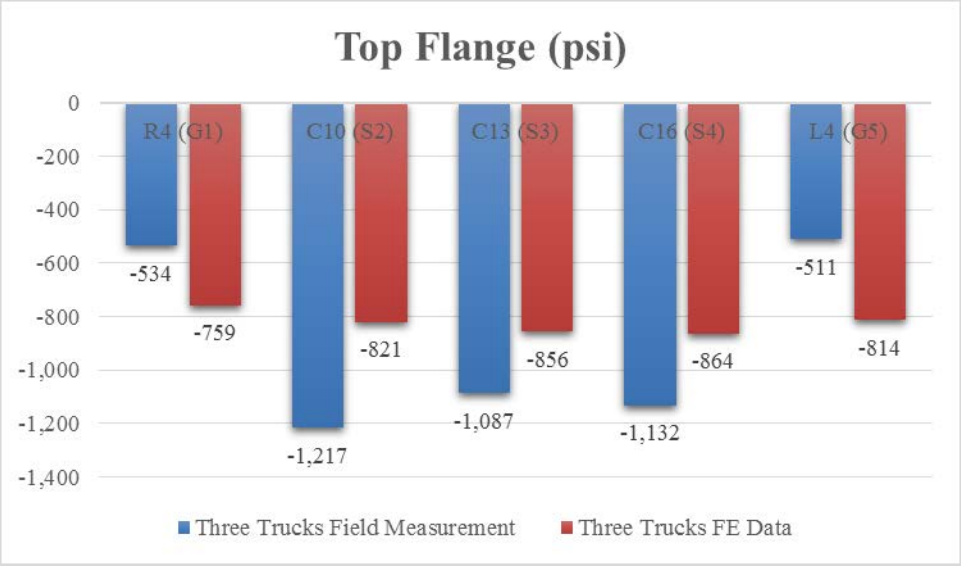

Figure 3.1 Top flange stress comparison between field measured and calculated values (psi)

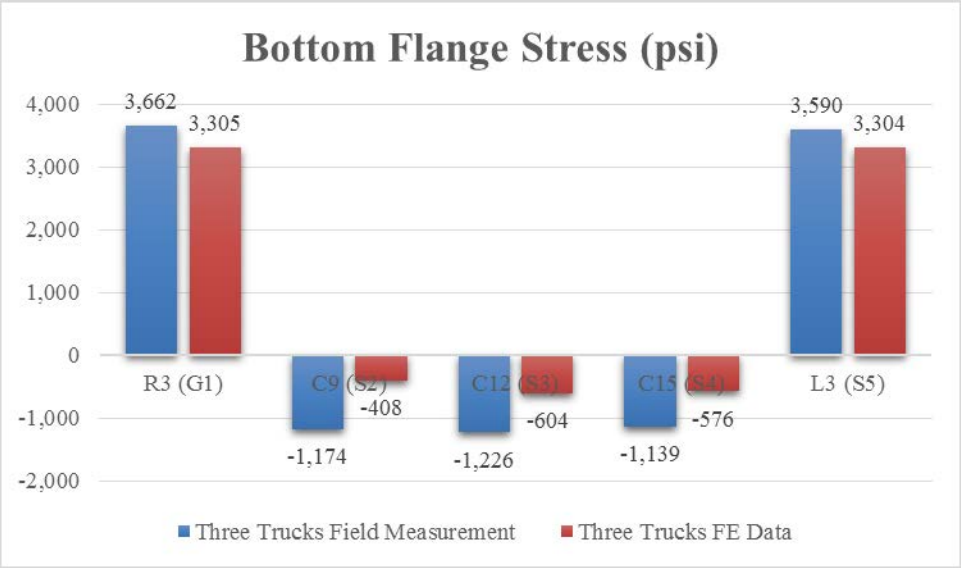

Figure 3.2 Bottom flange stress comparison between measured and calculated values (psi)

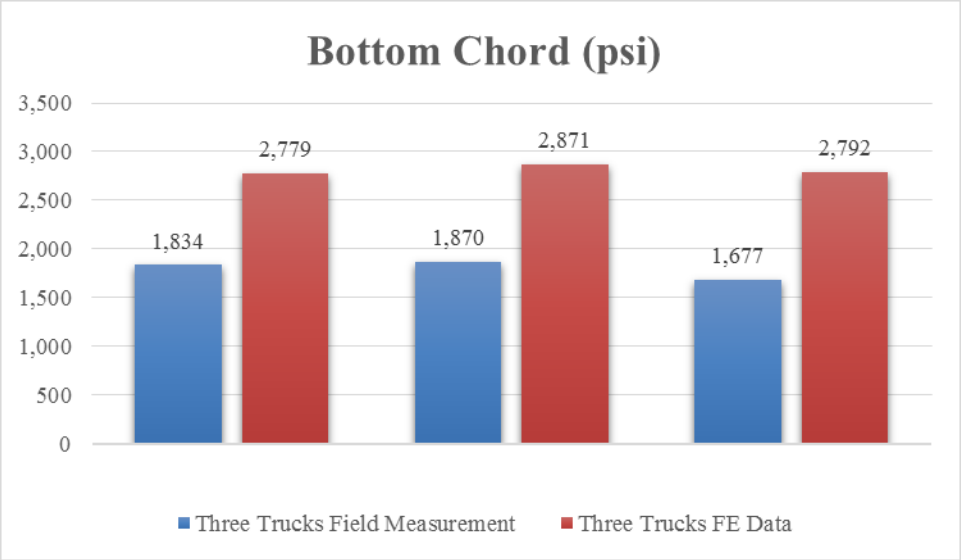

Figure 3.3 Lower chord stress comparison between measured and calculated values (psi)

CHAPTER 4.0 MODEL IMPROVEMENTS IN THE LONGITUDINAL DIRECTION

Initially, we identified the members that were likely to affect structural response the most. In selecting objective functions for study, we adjusted member sectional data and member geometry to better reflect the 1993 as-built construction. According to the longitudinal behavior described by the unmodified HDR FEM, the largest error exists in a lower chord member. Modifications showed that if the cross-sectional area in the lower chord was reduced to 0.43, the resulting error in local strain dropped below 50%. This modification resulted in a change in behavior, and the largest error between measured and calculated stresses was now in the composite truss lower flange. We than investigated the bridge response to a change in stiffness for the concrete deck. Changing the elastic modulus of the concrete deck to 3,000 ksi improved structural response, and the error between the calculated and measured stresses were reduced to 5%. However, the difference between the global experimental frequency response and calculated values causes the percent error to increase to 15% (that is, the stiffness change went from too stiff to too flexible). In order to balance the difference in error between local and global values, the elastic modulus of the concrete deck was changed to 3,300 ksi and the stringer lower flange area was changed from 2.0 to 2.5. The change in area represents the actual area shown on the as-built construction drawings. Table 4.1 shows the influence of these modifications on structural response. Tables 4.2, 4.3, and 4.4 show the longitudinal difference between experimental and calculated stresses for both global and local values.

Ignoring signs, the largest error for the global values decreased from -10.2% to 8.8%, and the largest error for the local values decreased from -66.4% to -17.8% in the longitudinal

direction. The global measured data are from an ambient test, and the local data are based on the 13 fiber-optic strain sensors near the middle of Span 3.

Table 4.1 FEM using revised variables

Bridge Sections	Locations	Property Modifiers	
Composite Trusses	3 Lower Chord	Area	0.43
Girders	2 Top Flange	Area	0.54
	2 Bottom Flange	Area	0.85
Stringer	3 Top Flange	Area	1.24
	2 Bottom Flange (No. 2,4)	Area	2.0
	Bottom Flange (No. 3)	Area	2.5
Concrete Deck	Throughout the deck	Elastic Modulus (ksi)	3,300

Table 4.2 Natural frequency differences after model revisions for longitudinal behavior

Mode	Field Measurement (Hz)	Long. Updated FEM (Hz)	Difference (%)
Longitudinal Mode 1	1.500	1.368	8.8
Longitudinal Mode 2	2.190	2.036	7.0
Vertical Mode 1	2.846	2.773	2.6
Vertical Mode 2	3.224	3.196	0.9
Vertical Mode 3	4.580	4.271	6.8
Transverse Mode 1	2.095	2.168	-3.5
Transverse Mode 2	2.346	2.325	0.9
Transverse Mode 3	2.782	2.683	3.6

Table 4.3 Difference in flange stress (%) after model revisions for longitudinal behavior

Load Case	Location	1	2	3	4	5
	Sensor Number	R3	C9	C12	C15	L3
Top Flange	Field Measurement	-12.4	-12.0	--17.8	-17.4	-12.0
	Updated FE Data					
Bottom Flange	Field Measurement	-6.7	1.2	11.7	5.7	-9.9
	FE Data					

Table 4.4 Difference in lower chord stress (%) after model revisions for longitudinal behavior

Load Case	Location	1	2	3
	Sensor Number	R3	C9	C12
Top Flange	Field Measurement	-3.8	-6.8	--14.0
	FE Data			

CHAPTER 5.0 TRANSVERSE BEHAVIOR PRIOR TO MODEL MODIFICATIONS

The stiffness of the cross frame and the condition of the supports determined load distribution in the transverse direction. In the report by HDR, Inc., five roller bearings did not fully connect with the superstructure, and HDR, Inc. removed those supports from their FEM (HDR, Inc. 2011).

During Phase 1 of this study, we placed five displacement sensors at those locations to measure the movement of the roller bearings in the vertical direction. In addition, we installed eight strain sensors in diagonal members to measure the reaction of the supports and the stresses in the cross frames.

For one of the load test cases conducted on September 10, 2012, three heavily loaded trucks traveling side by side crossed the bridge at low speed (Hulsey et al. 2012b). The vertical movement of the five displacement sensors is shown in Figure 5.1a–e. These graphs illustrate the response for an average of 50 data points over time for each of the five bearing locations.

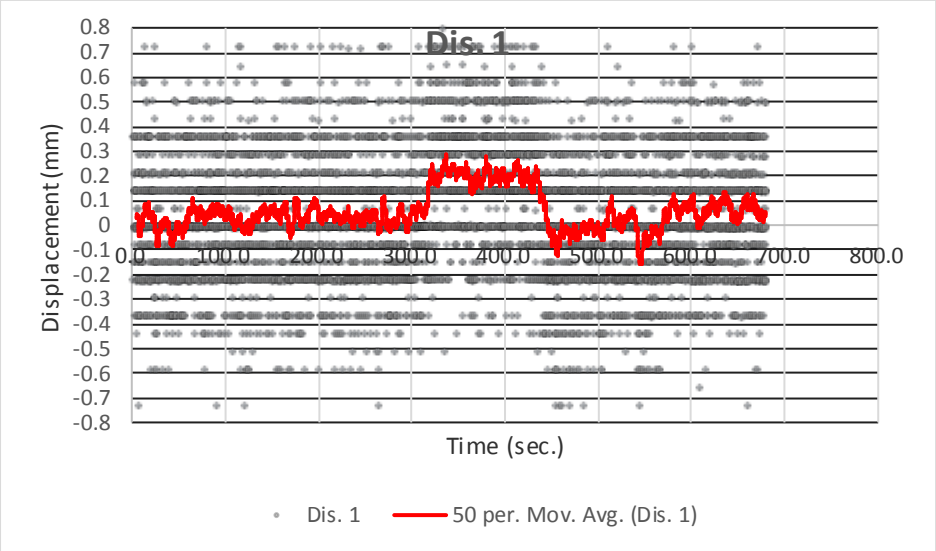

a. Vertical movement at displacement sensor 1

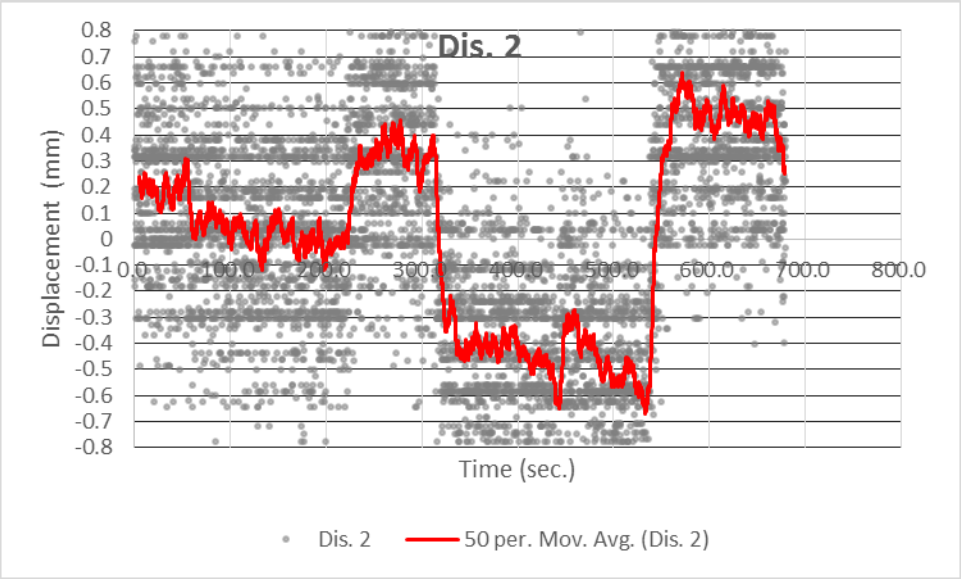

b. Vertical movement at displacement sensor 2

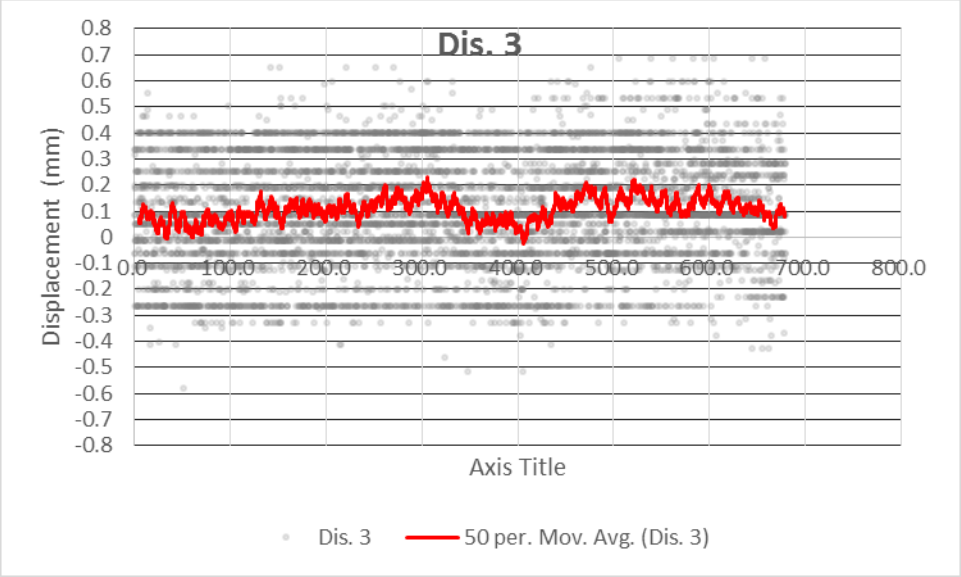

c. Vertical movement at displacement sensor 3

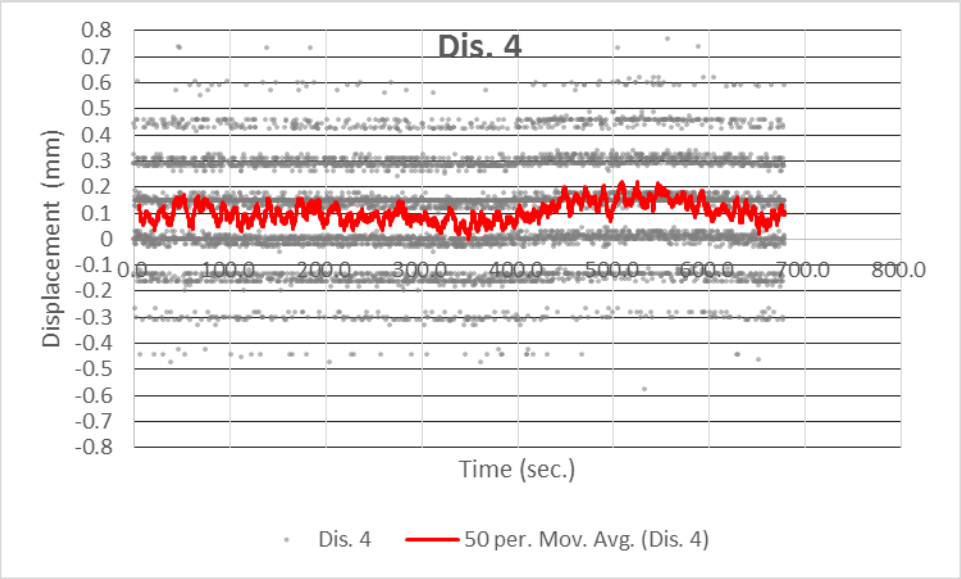

d. Vertical movement at displacement sensor 4

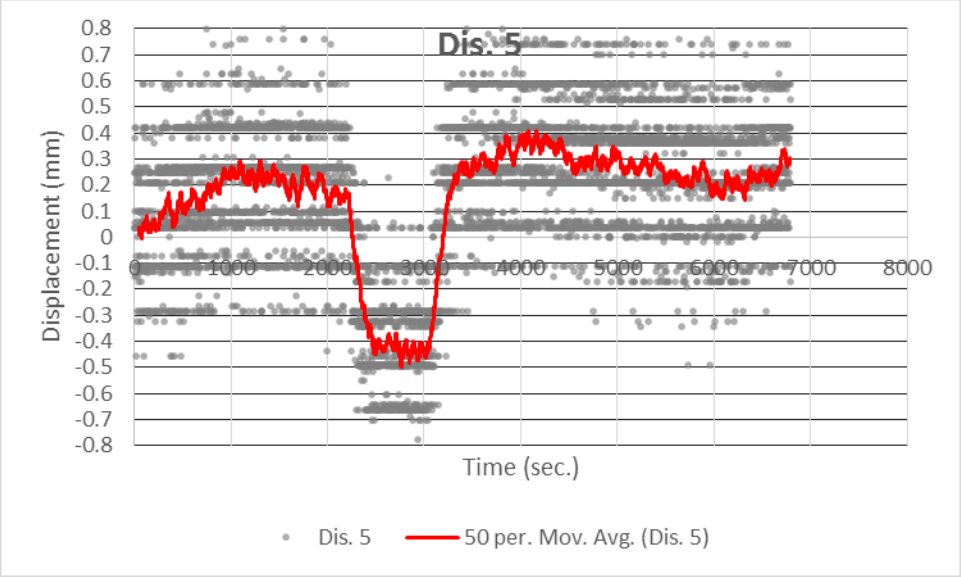

e. Vertical movement at displacement sensor 5

Figure 5.1 Vertical movement at 5 unconnected bearing supports

According to the displacement sensor results, roller bearings 1, 3, and 4 have limited movement in the vertical direction. When compared with the other roller bearings, bearings 2 and 5 are more flexible in the vertical direction than the others are.

In order to evaluate the distribution of reaction forces for a given load, eight strain sensors were installed (Phase 1) on the cross frame at the five unconnected roller support locations (Hulsey et al., 2012a). Tables 5.1 and 5.2 and Figures 5.2 and 5.3 show the stress results of measured and FEM stress before the model was updated. Table 5.1 and Figure 5.2 show the stress results when two parallel trucks stop above Pier 3. Table 5.2 and Figure 5.3 show stress results when two parallel trucks stop over Pier 5. The details of these load tests are presented in the AUTC Load Test Report (Hulsey et al. 2012b). Sensor numbers and their locations are presented according to the modifications that were made to the FEM in the transverse direction

Table 5.1 Two trucks at Pier 3, before transverse modifications

Location	C7	C6	C5	C4
Measured Stress (psi)	-2,237	1,127	1,726	-2,021
HDR FEM Stress (psi)	-2,963	1,482	1,466	-2,898
Error (%)	-32.4	-31.5	15.1	-43.4

Table 5.2 Two trucks at Pier 5 stress results before transverse updating

Location	C28	C27	C25	C24
Measured Stress (psi)	-2,171	-2,058	-376	-1,172
HDR FEM Stress (psi)	-2,184	-2,366	-2,305	-2,261
Error (%)	-0.6	-15.0	-512.3	-92.9

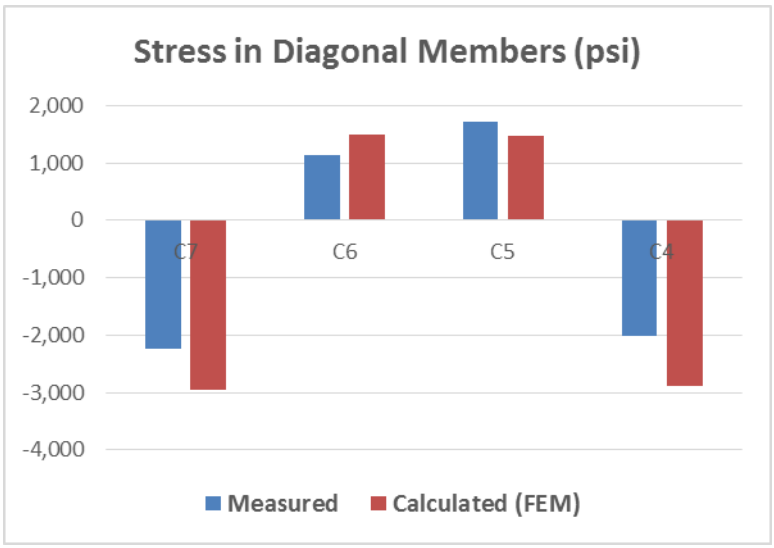

Figure 5.2 Two trucks at Pier 3 stress results before FEM transverse modifications

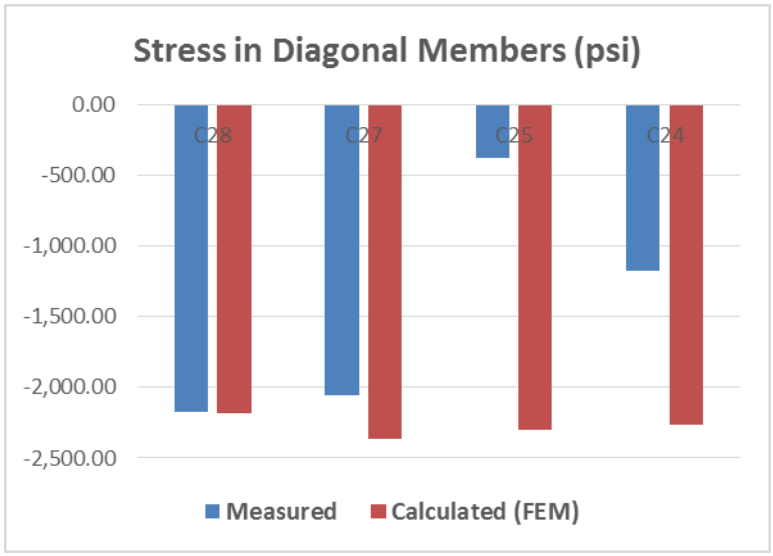

Figure 5.3 Two trucks at Pier 5 stress results before transverse updating

CHAPTER 6.0 MODEL IMPROVEMENTS IN THE TRANSVERSE DIRECTIONS

Figures 5.2 and 5.3 show for the 2012 load tests that large errors exist between measured and calculated stresses in the cross frame. At Pier 3, the largest error is -43.4% in the cross frame. At Pier 5, the largest error was -512.3%. Figure 5.1 indicates that bearings 1, 3, and 4 have limited movement. So the cross frame section may work as a semi-rigid support at those locations. As part of the model modifications, three spring supports were added at those locations. In order to reduce errors in the objective functions, we modified the support spring stiffness and sectional properties of the cross frame to more closely represent 1993 as-built conditions and behavior of this structure. Vertical spring support stiffness at locations 1, 3 and 4 are 1,200 kip/inch, 100 kip/inch, and 40,000 kip/inch, respectively. The cross frame truss section area was decreased to 0.8. The results for the modified FEM are shown in Tables 6.1 and 6.2 and Figures 6.1 and 6.2.

Table 6.1 Two trucks at Pier 3 stress results after model modificatons (psi)

	C7	C6	C5	C4
Measured Stress (psi)	-2,237	1,127	1,726	-2,021
FEM Stress (psi)	-2,419	1,002	1,560	-2,106
Error (%)	-8.1	11.1	9.6	-4.2

Table 6.2 Two trucks at Pier 5 stress results after model modifications (psi)

	C28	C27	C25	C24
Measured Stress (psi)	-2,171	-2,058	-376	-1,172
FEM Stress (psi)	-1,8301	-1,0813	-2,027	-946
Error (%)	11.3	-17.0	-19.9	19.3

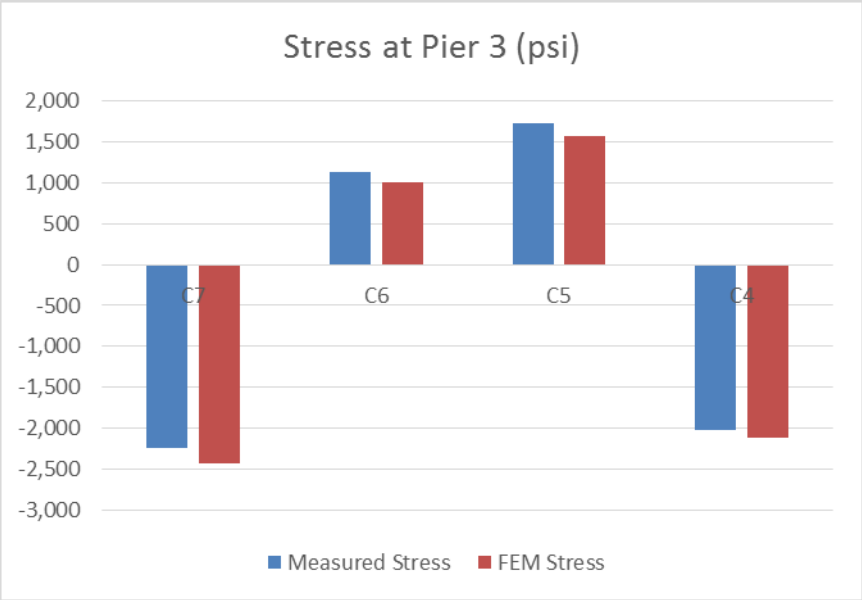

Figure 6.1 Two trucks at Pier 3 stress results after model modifications

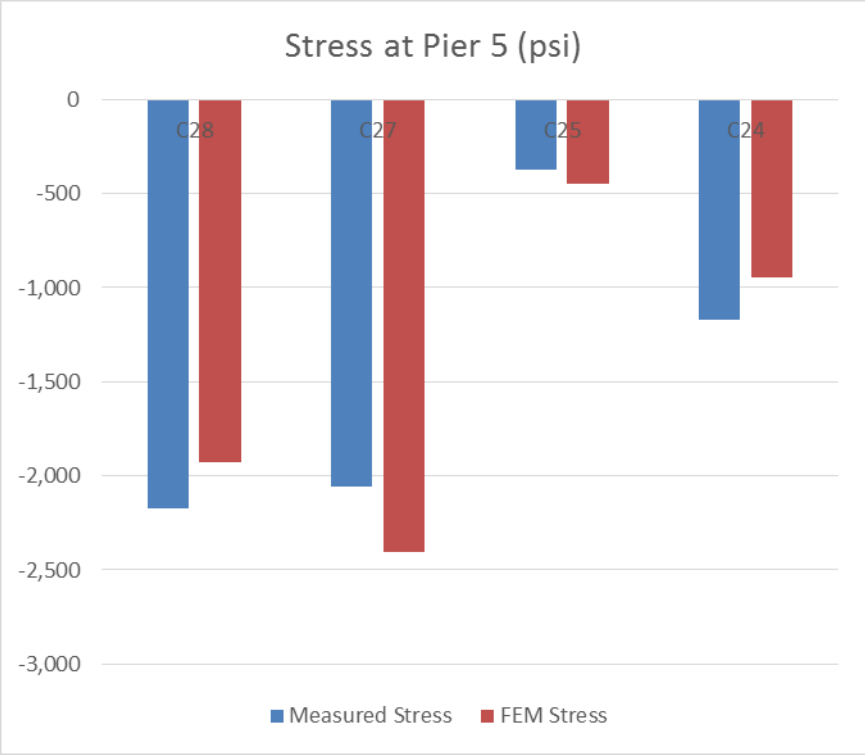

Figure 6.2 Two trucks at Pier 5 stress results after model modifications

Following modification of the model, the largest error in the transverse direction decreased from -512.3% to -19.9%. Initially, five support bearings did not support the bridge (i.e., the superstructure was not in contact with the bearings). After the model was modified, we simulated the bridge response with two bearings (Bearings 2 and 4) that were not in contact with the structure. At the other three bearing locations, the superstructure is modeled with vertical springs between the bearing support and the structure. The cross frames were found to be too stiff compared with the as-is condition.

After the FEM was modified to more accurately represent the transverse behavior of the bridge, a comparison between experimental and calculated stresses were made for the various load tests that were run on September 10, 2012. For example, Tables 6.3 and 6.4 show the difference in stresses between experimental and modified finite element values for the middle of the Span 3 girder flanges and the difference in stresses in the lower chord of the cross frame. These stresses are from a static load test in which three trucks side-by-side were on the bridge (see Figure 6.3). The tables show that the stiffness of the three spring supports and the cross frame had limited influence on the longitudinal distribution of load.

Table 6.3 Percent difference between FEM and experimental flange stresses mid-Span 3

Load Case	Location	1	2	3	4	5
	Sensor Number	R3	C9	C12	C15	L3
Top Flange	Field Measurement	-13.10	-13.50	-16.48	-17.69	-9.19
	FE Data					
Bottom Flange	Field Measurement	-6.58	0.71	5.43	4.26	-8.64
	FE Data					

Table 6.4 Percent difference between FEM and experimental lower chord stresses mid-Span 3

Load Case	Location	1	2	3
	Sensor Number	R3	C9	C12
Top Flange	Field Measurement	-2.77	-5.24	-12.67
	FE Data			

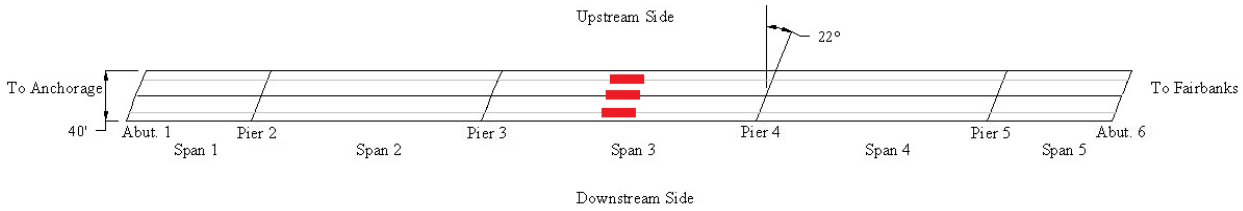

Figure 6.3 Three trucks positioned on Span 3, southbound

The FEM that resulted from modifications to better predict transverse response was evaluated for both local and global data. Using the improved model, global natural frequencies were calculated and compared with those that were measured with the portable accelerometers. Natural frequencies were calculated in three directions (vertical, longitudinal, transverse) and compared with the measured values (Table 6.5). The largest error was 8.9% for the first mode in the longitudinal direction. Based on a comparison between test data and calculated values, it is clear that the modified FEM is sufficiently accurate. We re-tested the Chulitna River Bridge to determine if a change in structural behavior may have occurred between 2012 and 2013. Table 6.6 illustrates that the bridge was stable during the year that we monitored its response.

Table 6.5 Year 2012 natural rrequency difference; calibrated FEM

Mode	Field Measured (Hz)	FEM Results (Hz)	Difference (%)
Longitudinal Mode 1	1.500	1.367	8.9
Longitudinal Mode 2	2.190	2.044	6.7
Vertical Mode 1	2.846	2.756	3.2
Vertical Mode 2	3.224	3.348	-3.8
Vertical Mode 3	4.586	4.249	7.3
Transverse Mode 1	2.095	2.269	-8.3
Transverse Mode 2	2.346	2.542	-8.4
Transverse Mode 3	2.782	2.788	-0.2

Table 6.6 Natural frequencies difference between 2012 and 2013

	2012 Ambient Test (Hz)	2013 Ambient Test (Hz)	FEM Calibrated Model
Longitudinal Mode 1	1.500	1.500	1.367
Longitudinal Mode 2	2.190	2.206	2.044
Vertical Mode 1	2.846	2.883	2.756
Vertical Mode 2	3.224	3.236	3.348
Vertical Mode 3	4.586	4.617	4.249

CHAPTER 7.0 CALIBRATED FINITE ELEMENT MODEL

A simple accuracy test was conducted to refine the mesh to ensure that it converged to a reasonable estimation of the response. The simple accuracy test results showed that the original HDR FEM had a mesh size that would provide an acceptable level of accuracy.

Next, we calibrated the FEM against structural response, which was done by modifying elements and structural properties to more accurately describe the as-built bridge structure. The modification process was divided into two stages: one in the longitudinal direction and the other in the transverse direction. Finally, the accuracy of the modified FEM was checked against structural response as measured by the sensors at the local level (the structural health monitoring system) and global level frequency response as measured with 15 portable accelerometers placed on the bridge deck.

Longitudinal members such as the girder flanges, stringer flanges, composite truss lower-chord cross area, and elastic modulus of the concrete deck were selected for study to determine if these items were accurately describing the as-built bridge structure. On September 10, 2012, three ADOT&PF dump trucks were used to load test the bridge; this was Phase 1. Static and dynamic strains, tilts, and displacements were measured for seventeen different combinations of truck positions. The measured local response data caused by these different load tests were compared with the FEM results; the differences between experimental and calculated data are the objective functions. Variables were selected and adjusted to match as-built construction drawings so that response was within a reasonable range.

The purpose was to reduce the objective functions; that is, the modeled geometry should be checked against as-built construction drawings. In addition to verifying that calculated local

strains were sufficiently accurate, we checked calculated global (vertical, longitudinal, transverse) natural frequencies against measured values. This check ensured that element and material property corrections for the model would result in convergence between measured and calculated.

In the transverse direction, the unconnected roller bearings and cross frames were selected for study. The transverse behavior was studied by evaluating load test response when two trucks were stopped at two critical cross sections. The difference between measured local strain values and calculated were evaluated and compared. The model was reviewed and modified to describe the as-built construction drawings. This process was continued until the model accurately described the behavior and the calculated values correlated well to the experimental values.

After model modifications, both local and global values resulted in lower errors between measured and calculated. For local values, the largest error decreased from -512.3% to -19.9%. For global values, the largest error decreased from -10.2% to 8.9%. The modified or refined (calibrated) FEM now provides calculated values with an accuracy that is within acceptable limits for both local and global values.

CHAPTER 8.0 A FUTURISTIC APPROACH TO CALIBRATING A FINITE ELEMENT MODEL

In the next stage of research, we will use an optimization method to modify and refine the model. Briefly, the FEM will be transferred into a mathematical model. More objective functions will be selected from static and dynamic tests. For the purpose of future research, we will begin with a FEM, and any changes will be referred to as model updates. As more variables are used and revised, it is appropriate to divide the structural system into small sections according to bridge spans. The objective functions and variables will be set within reasonable ranges. The optimized results will be calculated based on mathematical optimization methods. Additional objective functions and variables will ensure the reliability of the updated model. Our reasoning is that with this approach, an optimized updated method can be used to intelligently control the objective functions so that achieving convergence is reasonable and errors between experimental and calculated data will be small. After completing the FEM optimization scheme, the largest error between calculated and experimental data is expected to be between 2% and 5% for global values and between 5% and 15% for local values.

The outcome of this approach will be a FEM of the bridge's current condition. This model will provide a virtual behavioral response of the bridge for a given set of loading conditions. As more data are taken, the differences between experimental and calculated data should be routinely checked. If the bridge's latest measured experimental (SHMS) local data are different than predicted or if the latest measured global data are different, the health of the bridge has likely changed and a further investigation should be conducted.

CHAPTER 9.0 PROPOSED ALASKA BRIDGE MONITORING SYSTEM

The purpose of this chapter is to provide the reader with a clear plan for developing a structural health monitoring system for a given bridge in Alaska. Consider that it will be an objective to select the minimum number of sensors to describe bridge performance and, more importantly, to describe the bridge's response to typical traffic loads, special permit loads, and exposures such as snow, wind, ice forces, earthquakes, etc.

This section describes the minimum experimental system that is needed to evaluate the required bridge performance. We recommend that bridge behavior is evaluated at both the global level (macro response) and local level (micro response, such as strain at a point). This approach may look like the following:

- Provide a system to monitor bridge performance at the global level.
- Measure ambient accelerations at the time you perform a bridge inspection. This can be done by using a portable system that measures accelerations. Depending on the bridge, we recommend 15 to 20 portable accelerometers.
- Install a structural health monitoring system to monitor bridge response at the local level.
- Any system that involves measuring data over a long time requires careful consideration of sensor types. For example, it is critical that you have a system in which the sensors do not drift over time, and the sensors must be minimally affected by stray currents from power lines, etc.

- If you plan to study a structure for a long time, we recommend the following approach in developing a monitoring system:
    a) Monitor support reactions (find live load distribution).
    b) Use strain gauges to measure the behavior at critical points or at locations where there is some concern.
    c) Use pressure transducers to monitor backwall-induced pressures from the embankments.
    d) Use one or two accelerometers per span if you are in earthquake country or you are interested in dynamic forces that are imposed by traffic. This information will help you calibrate against the AAHTO impact factors.
    e) Install gap gauges at the top of the piers. This information will verify how the longitudinal breaking forces and other imposed horizontal forces are distributed to the structural system.
- New bridges: Install load cells at the bearings. This information will provide the bridge engineer with an understanding of the dead load per each support and the live load distribution for traffic and special permit loads. This approach will also provide the bridge engineer with an understanding of the load paths. A minimum number of additional sensors can be added to address possible changes in load paths within the structural framing system. This information will inform the engineer of change in the health of the structure. We also suggest that you measure the ambient vibrational response (global data) every two years when the bridge is being inspected.
- Existing bridges: If you are planning to monitor an existing bridge, the built-in dead load stresses are not known; however, you can accurately monitor the live load

distribution by providing sensors at members that frame into the support bearings. We also suggest that you measure the ambient vibrational response (global data) every two years when the bridge is being inspected.

- All bridges: Install strain gauges at critical points in your structure or at locations where you have concerns. At the time the bridge is inspected, we recommend that you monitor the natural frequency of the structure. This may be accomplished by placing between 15 and 20 portable accelerometers along the bridge centerline. As part of this effort, you should consider measuring the ambient vibrational response in the transverse, longitudinal, and vertical directions. This effort is quick, and the equipment can be part of the bridge inspection program.

CHAPTER 10.0 CONCLUSIONS

The purpose of this research effort was (1) to develop a finite element tool that could properly assess the Chulitna River Bridge for 1993 AASHTO Load Resistance Factor Design (LRFD) bridge loads and special permit loads and (2) to evaluate the level of stress that was being introduced into the bridge by truck traffic and special permit loads. In addition to studying the bridge's response to traffic, we studied the stress level caused by live loads. The history of how structural modifications were conducted to widen this bridge in 1993 was not found. Thus, the magnitude of the induced dead load stresses is not known.

Phase 1 (Previous Study)

Selection and installation of a Structural Health Monitoring System: In the spring of 2012, the AUTC research team selected a "Structural Health Monitoring System" (SHMS). This system uses fiber-optic sensors. The fiber-optic sensors were selected because of the long-term stability of this type of instrumentation. The research team then took a week-long course in theory, application, and installation of available fiber-optic sensor technology. We learned theory and we trained in the techniques of field installations and fiber splicing. Prior to sensor installation, the bridge was analyzed for AASHTO loads, and sensors were selected to assist in evaluating bridge health and to assist the research team in determining critical members. In late summer, Chandler Monitoring Systems (CMS) and the AUTC research team installed the SHMS.

Gravity load testing: On September 9, 2012, test trucks were measured and weighed. CMS calibrated the system, and the AUTC research team laid out the test plan for the following day. On September 10, 2012, we load-tested the bridge with seventeen different static and

dynamic load combinations of three heavily loaded dump trucks (2 bellies and a side dump) (Hulsey and Xiao 2013; Hulsey et al. 2012a, 2012b).

In all cases, the bridge was loaded using ADOT&PF dump trucks (two belly and one side dump). On September 9, 2012, the trucks were weighed and measured. During testing, static tests were performed by directing the drivers to position the front axles over a given location that we painted on the bridge deck prior to testing. Once wheels were in position, the trucks stopped, and the bridge allowed to quiet down, data were recorded.

Both static and dynamic tests were performed using three dump trucks (two belly dumps and a side dump). The test trucks are presented in Appendix A.

Ambient testing (2012 tests were Phase 1; 2013 tests were Phase 2): In addition to subjecting the bridge to truck loads, we also conducted ambient vibration tests in August 2012 and again in the summer of 2013. These tests are inexpensive and quick to conduct. For these tests, the bridge is excited, and we monitor the vibrational response (frequency) at 15 different accelerometers along the bridge centerline. The test conducted in August 2012 provides a baseline describing the health of this structure.

Phase 2 (Current Study)

In this study, SHMS local data were recorded between the end of September 2012 and December 31, 2013. System monitoring occurred remotely, in that the sensors could be monitored in real time from the researcher's office at the University of Alaska Fairbanks campus.

In addition to monitoring traffic loads, we conducted an ambient vibration test during summer 2012. This test was done by setting up 15 accelerometers along the bridge centerline and digitally recording global vibration data for longitudinal, transverse, and vertical excitations. The second ambient vibration test was conducted during summer 2013. This test provided a

determination of possible change of the bridge over that one-year period (this is like going to the doctor for a physical exam).

In this study, we attempted to calibrate a FEM to as-built conditions and evaluate the predicted HL-93 live load stresses. Comparisons between FEM calculated strain data and the local (SHMS) experimental data were made for the seventeen different September 10, 2012, load cases. The model was calibrated to measured global frequencies for this bridge. These data were recorded at two different times: August 2012 and May 2013. The calibrated finite model provides very good results for both local and global data. Based on these findings, the FEM could be confidently used to predict the behavior of the Chulitna River Bridge. Our findings show that member live load stresses for the bridge are low. Dead load stresses for the interior truss girder are high, but not defined. The study had three conclusive outcomes:

Outcome 1 – Finite element model

- We have a finite element model that is now calibrated against two different data sets: measured ambient frequencies (global data) and SHMS (local strain) data. The results are satisfactory, and the model can be reliably used to evaluate bridge response such as HL-93 AASHTO loads and special permit loads that will be traveling across the Chulitna River Bridge.

Outcome 2 – Structural evaluation and load rating

- We load-rated the bridge for two different conditions: One is the existing condition and the other is based on modifying the bridge so that load is carried by all the support bearings. Between one and four members did not pass the required bridge load rating of ≥ 1. These members are on the lower section of the interior truss girder

near the bearing supports that are not in contact with the superstructure (see Appendix C).

Outcome 3 – LRFR HL-93 Live load stresses for the critical members

- Member stresses in three of the four interior truss girder members near the bearing supports not in contact with the superstructure have calculated dead load stresses that were around 50% of member capacity. If the gap (separation) between the five bearing supports and the superstructure occurred during construction widening and strengthening, there is low probability that the stresses in these members are this high. Depending on the construction sequence, it is likely that the exterior girders picked up most of the dead load. The answer to how the construction widening occurred may be in the ADOT&PF archives and should be investigated.

REFERENCES

HDR, Inc. 2011. “Load Rating and Structural Assessment Load Rating Report – Bridge No. 255: Chulitna River Bridge.”

Hulsey, J.L., and F. Xiao. 2013. “Mid-span Loading Report.” Alaska Department of Transportation Research, Development, and Technology Transfer, Fairbanks, Alaska.

Hulsey, J.L., P. Brandon, and F. Xiao. 2012a. “Structural Health Monitoring and Condition Assessment of Chulitna River Bridge: Sensor Selection and Field Installation Report.” Alaska Department of Transportation Research, Development, and Technology Transfer, Fairbanks, Alaska.

Hulsey, J.L., P. Brandon, and F. Xiao. 2012b. “Structural Health Monitoring and Condition Assessment of Chulitna River Bridge: Load Test Report.” Alaska Department of Transportation Research, Development, and Technology Transfer, Fairbanks, Alaska.

Hulsey, J.L., F. Xiao, and G.S. Chen. 2013a. “Structural Health Monitoring of an Alaska Bridge.” *6th International Conference on Structural Health Monitoring of Intelligent Infrastructure*, Hong Kong, December.

Hulsey, J.L., F. Xiao, and G.S. Chen. 2013b. “Structural Health Monitoring System Optimization for A Bridge.” *6th International Conference on Structural Health Monitoring of Intelligent Infrastructure*, Hong Kong, December.

Xiao, F., G. S. Chen, and J.L. Hulsey. 2012. “Experimental Investigation of a Bridge Under Traffic Loadings.” *International Conference on Frontiers of Mechanical Engineering, Materials and Energy (ICFMEME 2012)*, Dec. 20, Beijing, China.

Xiao, F., G.S. Chen, and J.L. Hulsey. 2014. “Experimental investigation of a bridge under traffic loading.” *Advanced Materials Research*, 875–877: 1989–1993.

Appendix A – Correlation between Calibrated Model and Experimental

Mid-Span 2 Static Load Test with Three Trucks

Three trucks were stopped side by side near the middle of Span 2. Strain sensors C3, C2, and C1 on the lower chords for the interior truss girder in Span 2 are presented for review and consideration. A small sample of the load tests is presented in Appendix B; details are presented elsewhere (Hulsey and Xiao 2013; Hulsey et al. 2012b). These tests illustrate the correlation between the calibrated model and experimental data. Sensor locations can be seen on the sensor layout presented in Appendix D. Table A.1 and Figure A.1 show FEM local stresses and calculated local stresses from the measured local strains for a three-truck load test. These data show that errors for the selected samples presented herein are small.

Table A.1 Difference in mid-Span 2 loading condition

	C3	C2	C1
Measured Stress (psi)	2,006	1,994	2,091
updated FEM Stress (psi)	2,056	2,090	2,030
Error (%)	-2.5	-4.8	.9

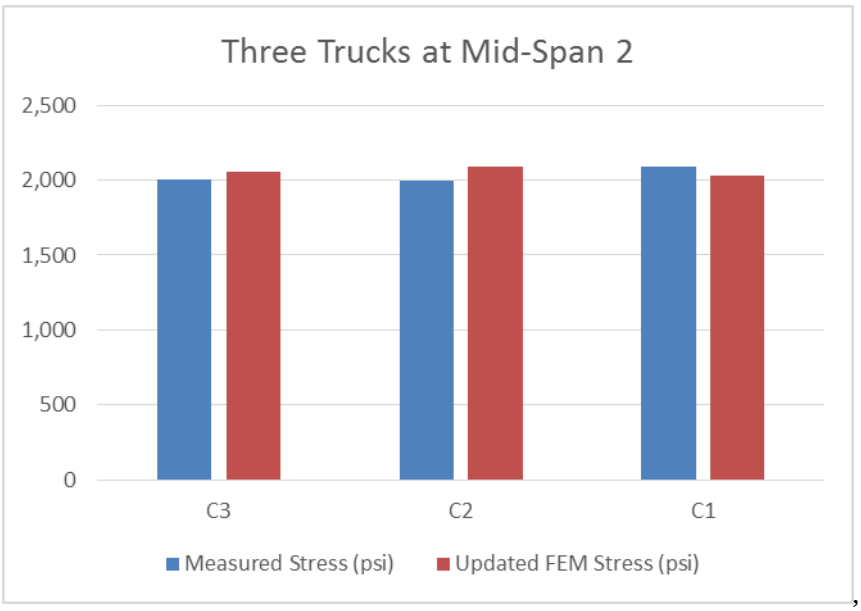

Figure A.1 Stress results in mid-Span 2 loading condition (psi)

Mid-Span 4 Loading Condition

Table A.2 Difference in mid-Span 4 three trucks side-by-side

	C23	C22	C21
Measured Stress (psi)	1,763	1,646	1,727
Updated FEM Stress (psi)	1,834	1,910	1,883
Error (%)	-4.0	-16.0	-9.0

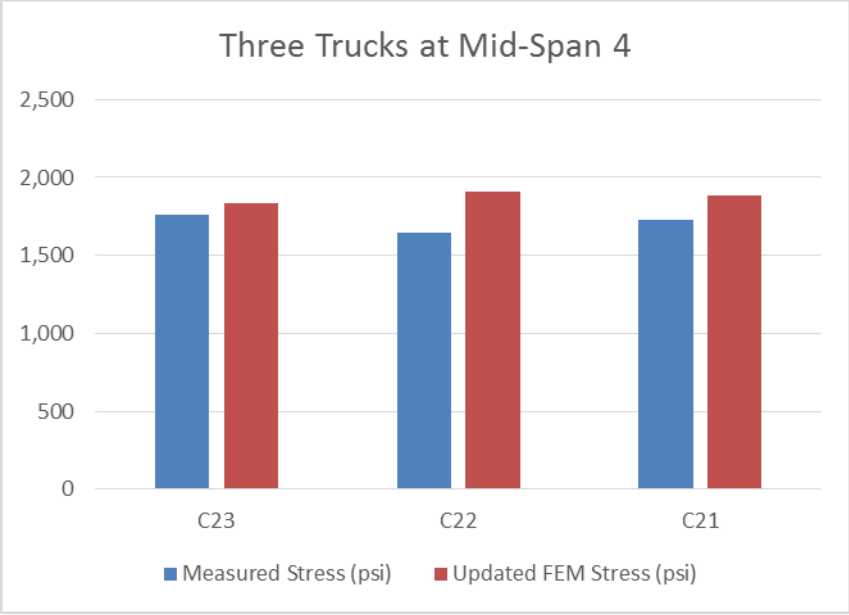

Figure A.2 Stress results for mid-Span 4 loading condition (psi)

Appendix B – Calibrated Finite Element Model

It is the purpose of this section to provide the reader with a three-dimensional view and details regarding the calibrated finite element model and its ability to virtually simulate the bridge response to load. The structure is 790 feet long; the bridge deck is 42 feet 2 inches wide. The bridge has 5 spans and is on a 22-degree skew. The model, which is shown in Figure B.1, uses SAP 2000 as the computer program; it has 4,697 nodal points, 4,615 frame elements, and 2,925 areas. Table B.1 shows the number of elements that were used to accurately describe the current condition of this bridge. Tables B.2 and B.3 provide some of the known details about the bridge supporting system.

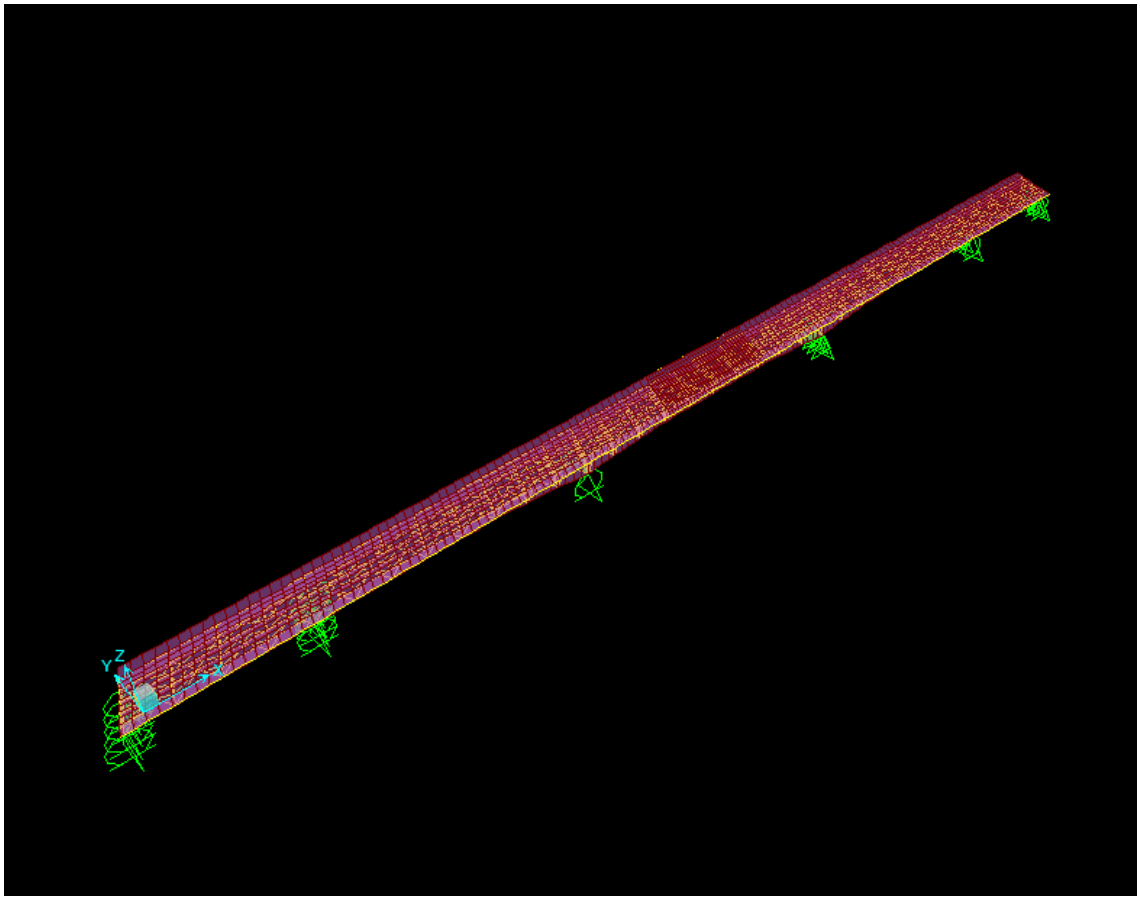

Figure B.1 Three-dimensional finite element model

Table B.1 Types of elements used in the model

Section		Element Type
Deck		Shell
Truss		Frame
Stringer	Web	Shell
	Flange	Frame
Girder	Web	Shell
	Flange	Frame

Table B.2 As-built support condition

	Abutment 1	Pier 2	Pier 3	Pier 4	Pier 5	Abutment 6
West Girder	Roller	Roller	Rollers	Fixed	Roller	Roller
West Truss	Roller	Roller	Roller	Fixed	Roller	Roller
Center Truss	Roller	Roller	Roller	Fixed	Roller	Roller
East Truss	Roller	Roller	Roller	Fixed	Roller	Roller
East Girder	Roller	Roller	Roller	Fixed	Roller	Roller

Table B.3 Calibrated FEM support condition

	Abutment 1	Pier 2	Pier 3	Pier 4	Pier 5	Abutment 6
West Girder	Roller	Roller	Rollers	Fixed	Roller	Roller
West Truss	Roller	Roller	100 kips/in	Fixed	Unconnected	Roller
Center Truss	Roller	Roller	Unconnected	Fixed	Roller	Roller
East Truss	Roller	Roller	1200 kip/in	Fixed	40,000 kips/in	Roller
East Girder	Roller	Roller	Roller	Fixed	Roller	Roller

Note: Bearing supports with a gap

Location 1: Spring support stiffness is 1200 kip/inch in vertical direction.
Location 3: Spring support stiffness is 100 kips/inch in vertical direction.
Location 4: Spring support is 40,000 kips/inch in vertical direction.
Locations 2 and 5: At these locations, the bridge is not connected to the supports.

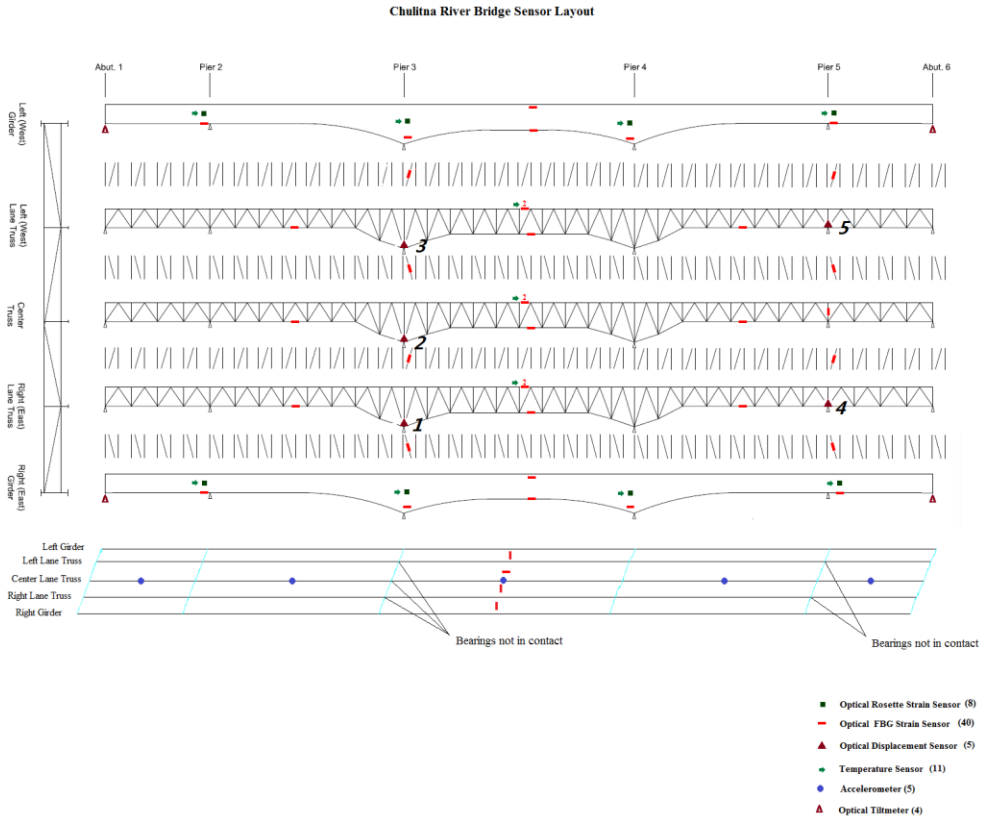

Figure B.2 Sensor layout and location for five bearing supports with a separation

Appendix C – Bridge Load Rating

General

The bridge was rated based on the LRFR method according to the AASHTO "Manual for Bridge Evaluation," 2011. The girders, composite trusses, and cross frame were rated in this study. The bridge was rated for a calibrated finite model by the Alaska University Transpiration Center (AUTC). The model was calibrated with two different experimental data sets and the as-built construction drawings. What is not known are the built-in dead load stresses resulting from the bridge widening and strengthening activities that occurred in 1993.

Load Rating

The member dead load stresses are considered to be carried by the members as if the structural framing had been in place before the deck and railings were installed. We choose the strength limit state for load rating in that it is the primary limit state in load rating. The load rating, which includes HL-93 inventory load rating and permit load rating, is summarized below for review and comment. The following conditions were considered during the load-rating process:

Three Lane (bridge driving lane is 42′ 2″)

HL-93 Inventory Load Rating (as-is condition)
HL-93 Inventory Load Rating (inserted bearing plates under the 5 separated rocker bearings)

Two Lane

HL-93 Inventory Load Rating (as-is condition)
HL-93 Inventory Load Rating (inserted bearing plates under the 5 separated rocker bearings)

One Lane

Permit Load Rating (as-is condition).

For permit load rating, only one heavily loaded truck was used. This information was provided by Bridge Design at ADOT&PF. The truck was the only traffic allowed on the bridge; it crossed the bridge along the centerline each time. This heavily loaded truck's axle distance and axle weight are shown in Table C.1.

Load rating results are provided in Table C.2 and Figures C.1 to C.4. These figures serve as a visual summary of the critical rating and of location on the structure. Members with a rating factor below 1.0 are displayed in red. All other members are performing satisfactorily.

Table C.1 Special permitted vehicle axle width is 21 feet.

Truck 1	Axle Load (kips)	16.9	28.45	28.45	34.92	34.93	33.15	33.15	31.18	31.17	30.5	30.25	32.22	32.22
	Axial Distance (ft)	0	23	5	15.5	6.08	14.5	4.42	99.75	4.42	13.5	4.4	14.42	4.42
Truck 2	Axle Load (kips)	16.8	29.025	29.025	34.725	34.725	33.025	33.025	31.75	31.75	30.825	30.825	32.6	32.6
	Axial Distance (ft)	0	23	5	15.6	6	14.6	4.5	99.9	4.5	13.3	4.5	14.6	4.5

Table C.2 A summary of the load ratings for the Chulitna River Bridge

Critical Locations	**A**	**B**	**C**	**D**
Member Sizes	2L6x4 ½ x 3/8	2L4x3 5/16 x 3/8	2L4x3 5/16 x 3/8	2L6x4 ½ x 3/8
Load Ratings:				
As-is: 3 lanes; HL-93	0.36	0.63	0.64	0.68
As-is: 2 lanes; HL-93	0.38	0.65	0.74	0.68
As-is: 1 lane; permit	0.59			
Supported: 2 lanes; HL-93			0.83	

Note: All other major load-carrying members had a satisfactory rating of ≥ 1.
"Supported" means that we considered all rocker bearings to be in contact with the interior truss girder. This means the 5 rocker bearings would be adjusted to make contact for a no-traffic condition.

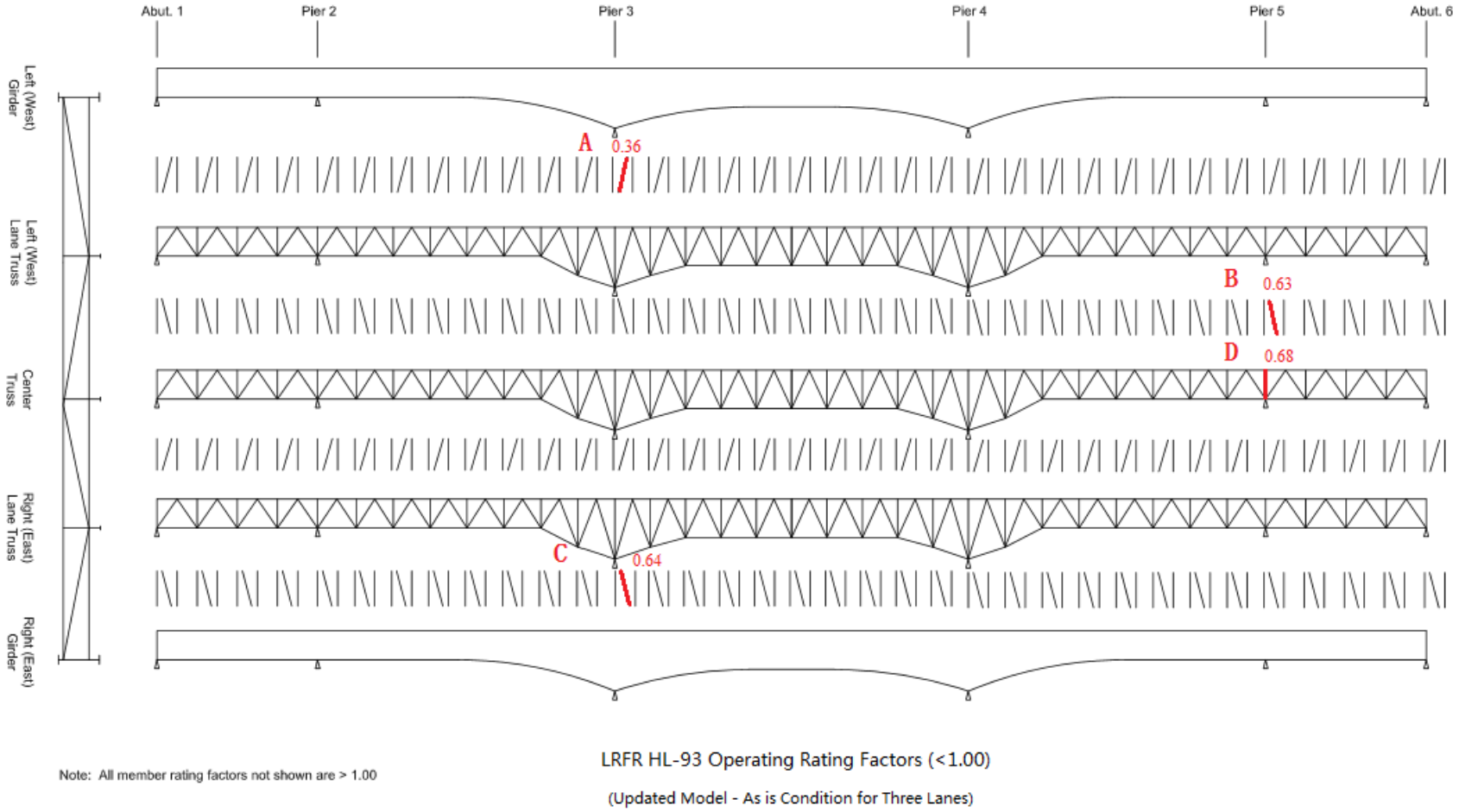

Figure C.1 Load rating: three lanes, HL-93, as-is

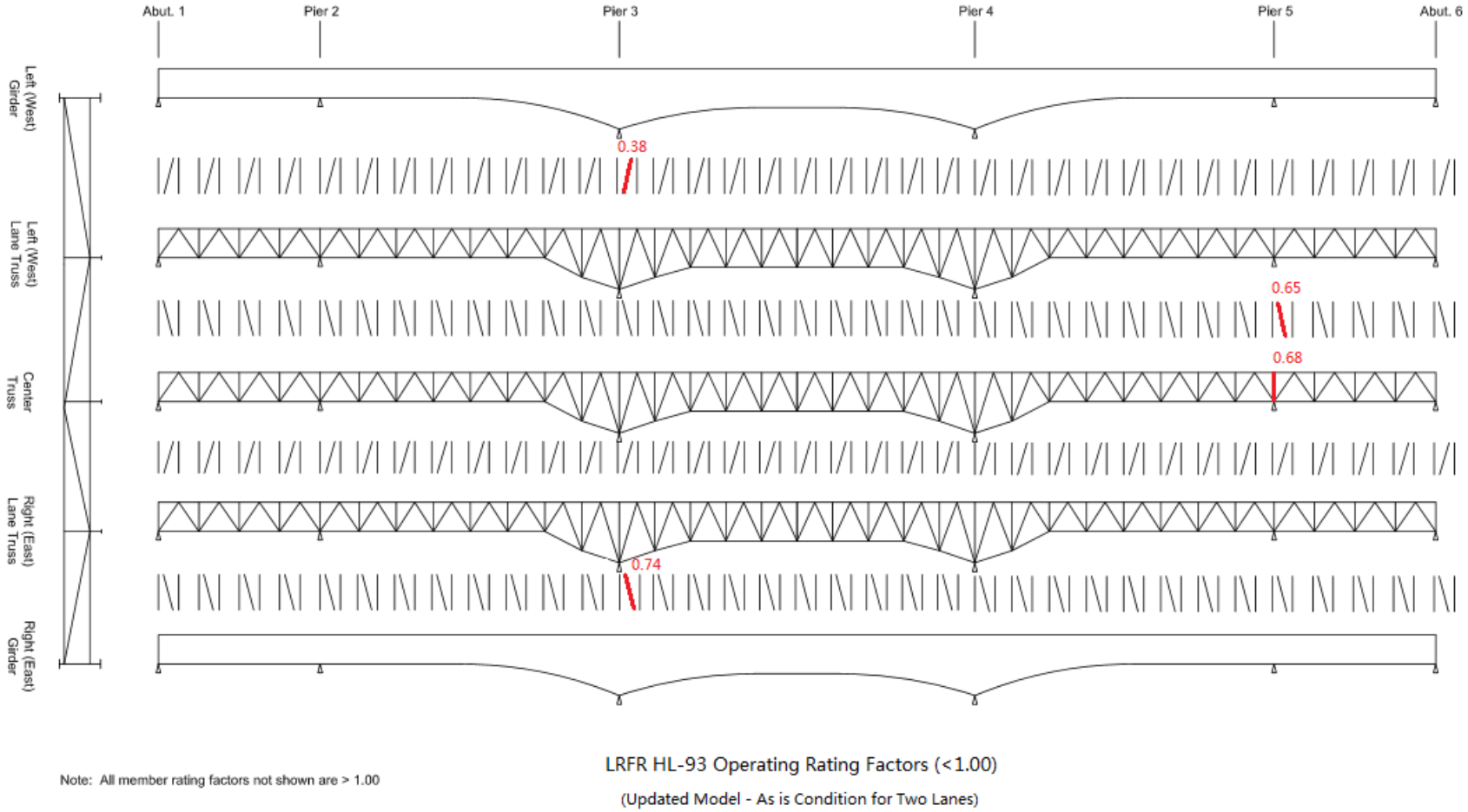

Figure C.2 Load rating: two lanes, HL-93, as-is

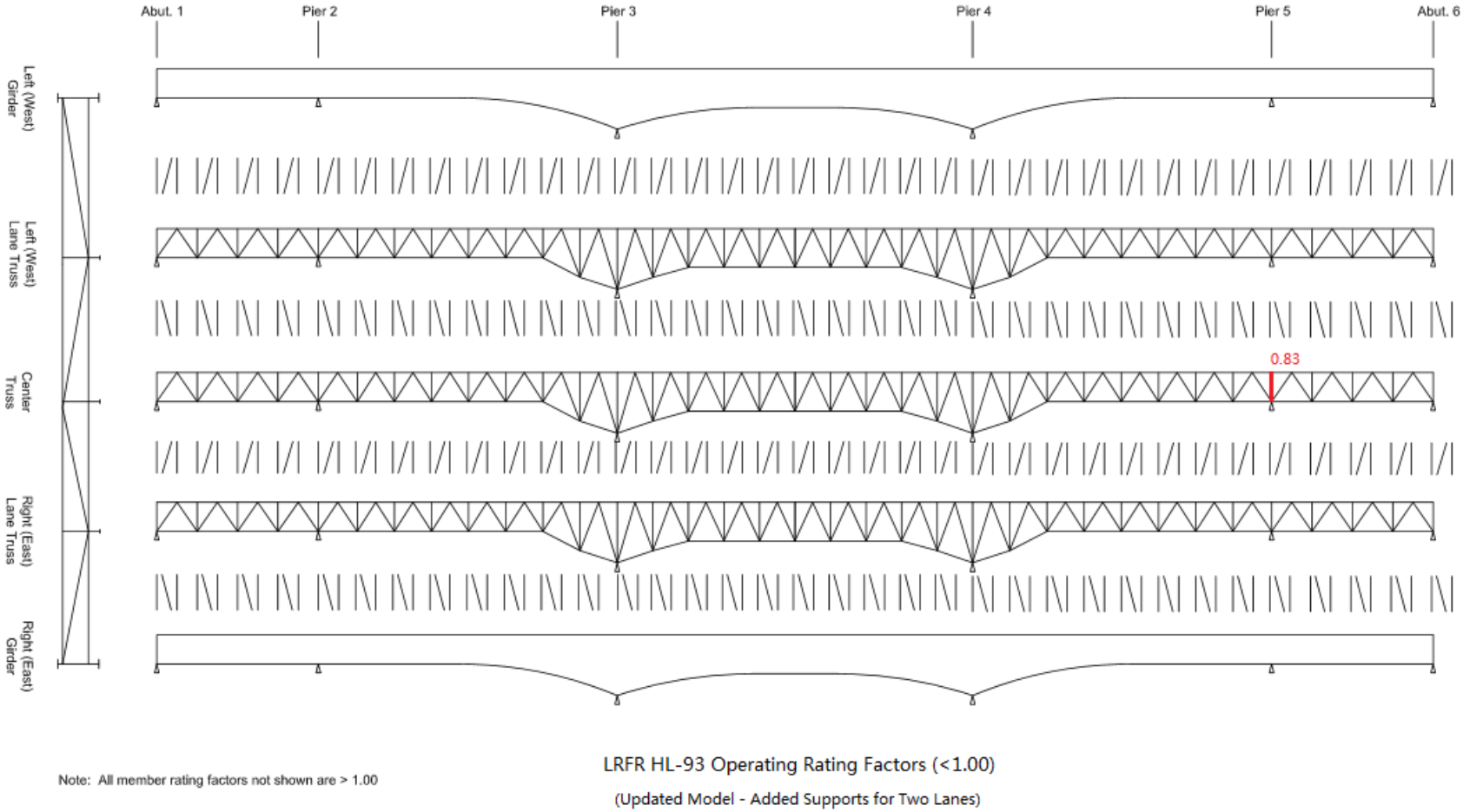

Figure C.3 Load rating for two lanes with all rocker bearings in contact

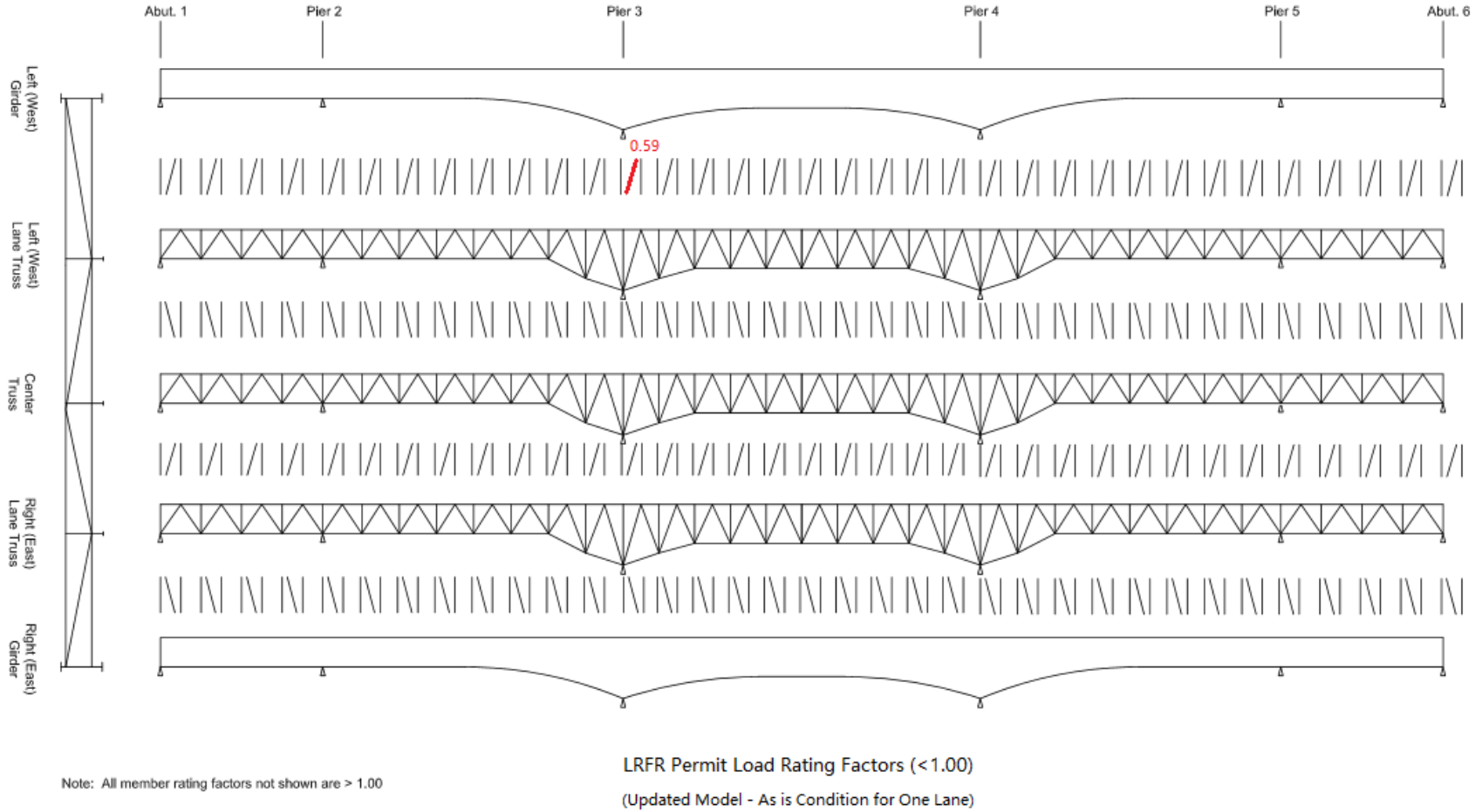

Figure C.4 Permit load on one lane over the existing bridge

Load Response for the Critical Members

Based on the load rating results, four members have a load rating below 1. The dead-load and live-load states of stress values for the HL-93 inventory load (three lanes) are shown in Table C.3. The member locations are in accordance with Figure C.1, which is identified as the figure named HL-93 inventory load rating (as-is condition three lanes).

Table C.3 HL-93 Inventory load (envelope for three lanes as-is condition)

Location	A	B	C	D
Frame	2L6x4 ½ x 3/8	2L4x3 5/16 x 3/8	2L6x4 ½ x 3/8	2L4x3 5/16 x 3/8
Area (in2)	9.5	4.1797	9.5	4.1797
Length (in)	173.3	110.8	173.3	63.8
Capacity (ksi)	-16.74	-19.94	-16.74	-24.86
Dead Load (ksi)	-10.07	-9.16	-8.08	-9.91
Live Load (ksi)	-8.42	-10.02	-7.63	-13.51
Load Rating	0.36	0.63	0.64	0.68

Appendix D – Sensor Layout

The structural health monitoring system chosen for the Chulitna River Bridge had 73 sensors that were selected in collaboration with ADOT&PF Bridge Design. The sensor layout was to assist in evaluating the load distribution through the structure. Details of the sensor layout are published elsewhere (Xiao et al. 2012). Figure D.1 and Table D.1 shows the sensor layout used to study the response of this bridge.

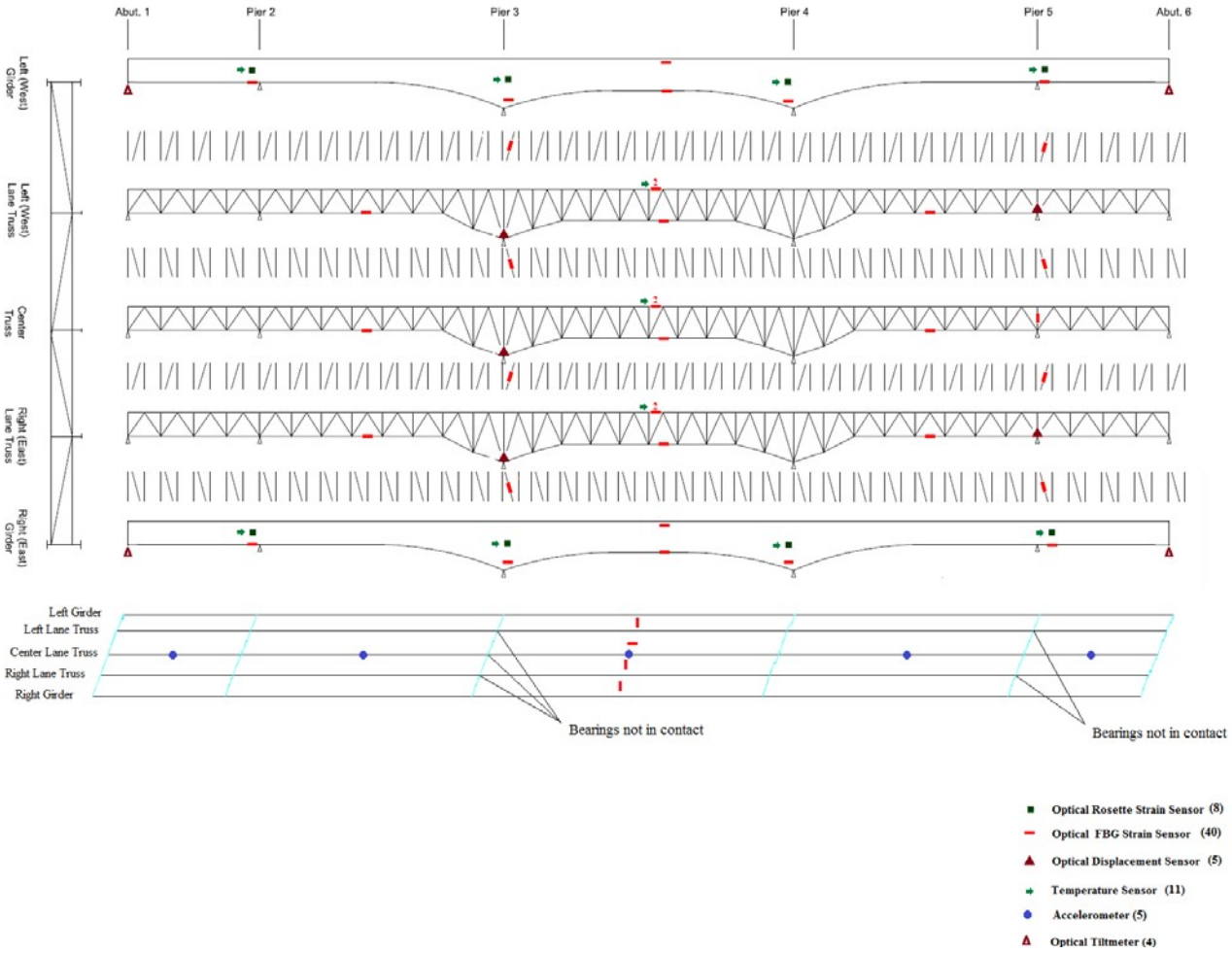

Figure D.1 Sensor layout

Table D.1 Summary of sensors

Sensor and Locations	Number of Sensors
Rosette Strain sensors	8
Strain Sensors on the Girders	12
Strain Sensors on the Composite Trusses	16
Strain Sensors on the Concrete Duck Strain	4
Sensor on the Diagonal Members	8
Accelerometers	5
Displacement Sensors	5
Temperature Sensors	11
Tilter meters	4
Total	73

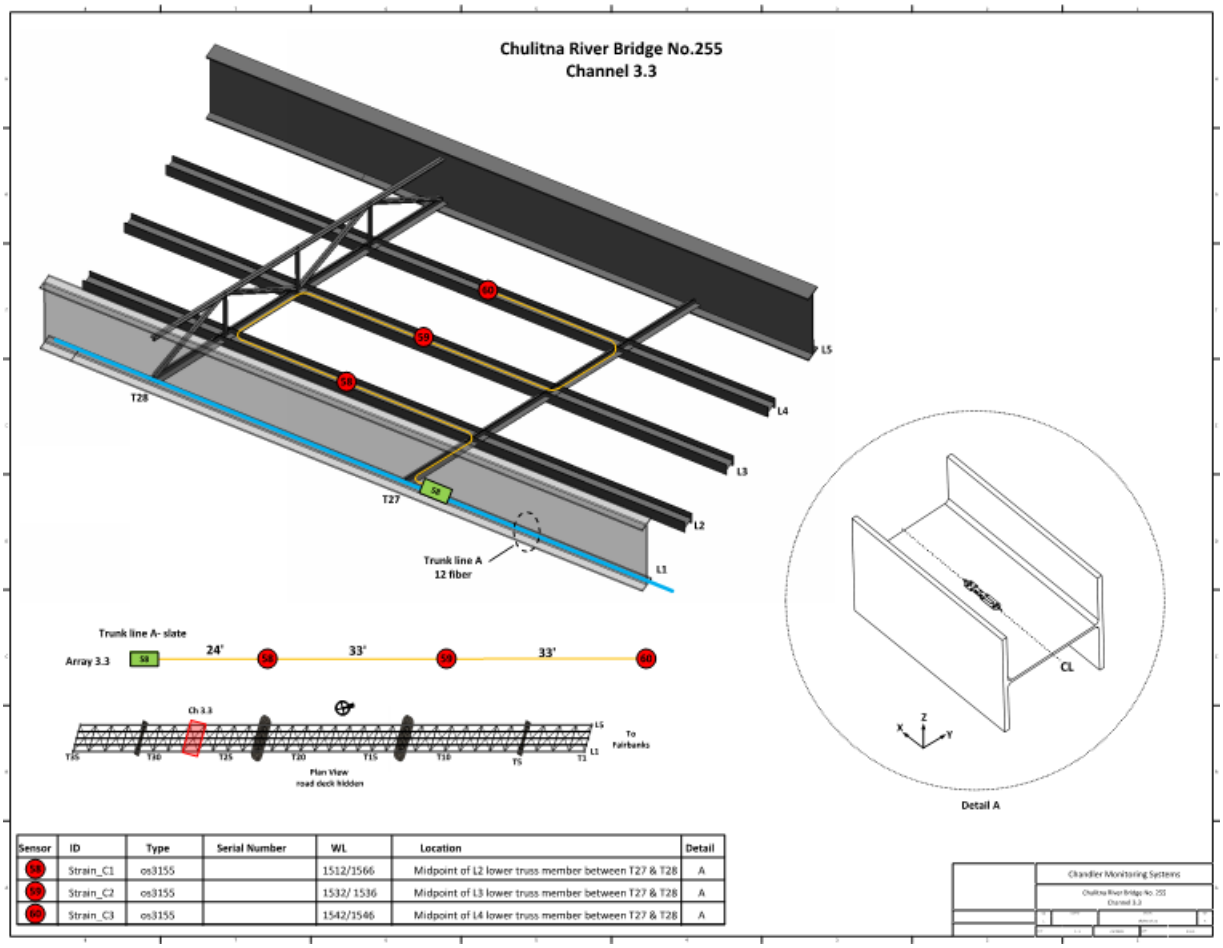

Figure D.2 Sensor layout providing strains in C1–C3

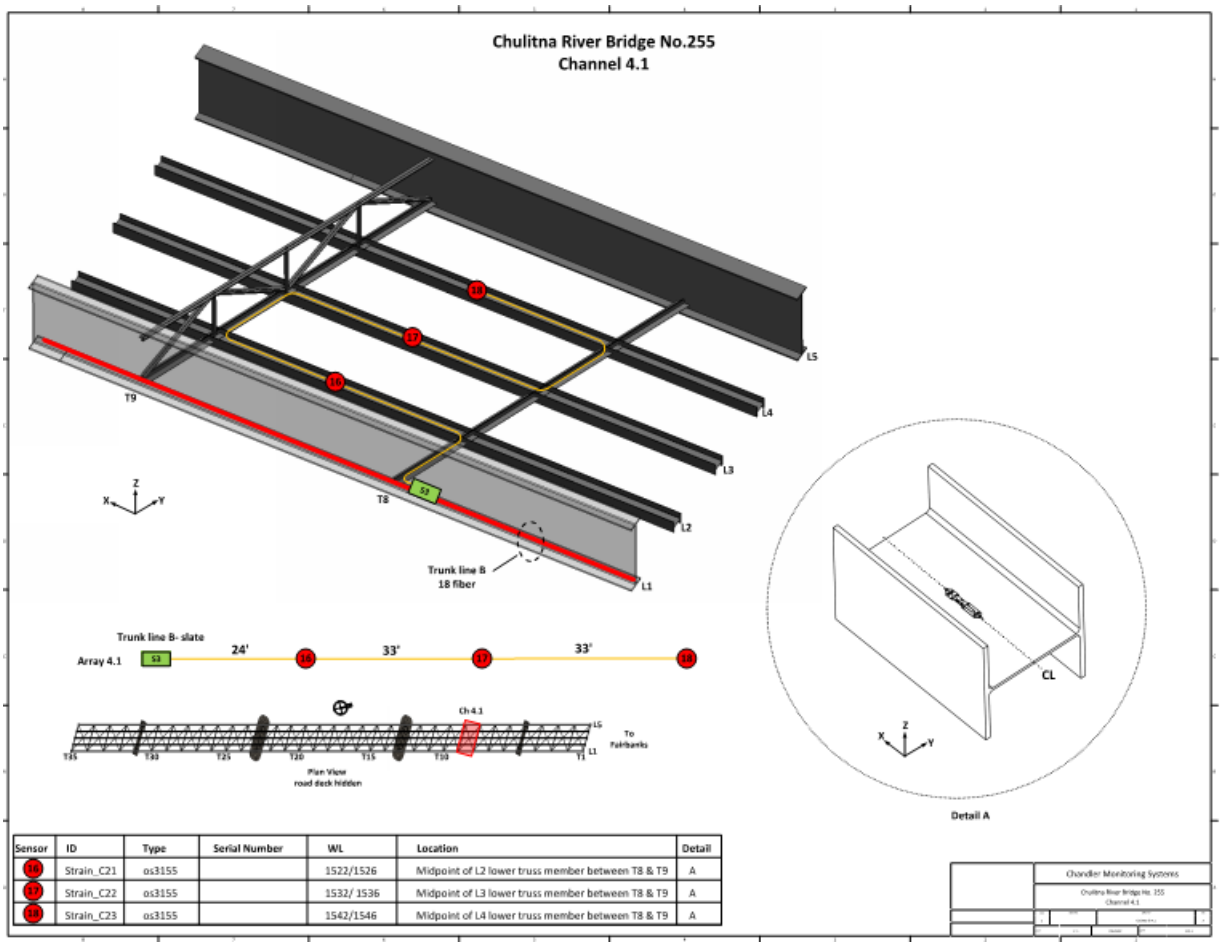

Sensor	ID	Type	Serial Number	WL	Location	Detail
16	Strain_C21	os3155		1522/1526	Midpoint of L2 lower truss member between T8 & T9	A
17	Strain_C22	os3155		1532/ 1536	Midpoint of L3 lower truss member between T8 & T9	A
18	Strain_C23	os3155		1542/1546	Midpoint of L4 lower truss member between T8 & T9	A

Figure D.3 Sensor layout providing strains in C21–C23

Appendix E – Load Testing

A finite element model of the Chulitna River Bridge was calibrated to Phase 1, September 2012 experimental truck load data; August 2012 Phase 1 ambient vibration test data, and May 2013 Phase 2 ambient vibration test data. The details of the 2012 loads are reported elsewhere (Xiao et al. 2012; Hulsey et al. 2012b; Hulsey et al. 2013a, 2013b; Xiao et al. 2014).

The tests selected to calibrate the bridge behavior were as follows:

- Phase 1 – August 2012 Ambient tests to find global frequency data
- Phase 1 – September 10, 2012, load tests
  - Local data from the two truck static loading (Trial 1);
  - Local data for the three truck static loading (Trial 17); and
  - Local data for the three truck dynamic loading (Trial 6);
- Phase 2 – May 2013 Ambient tests to find global frequency data

Appendix E is presented to provide the reader an understanding of the data used to calibrate the finite element model.

Phase 1

Global test data: In August 2012, “ambient” tests were conducted to evaluate the natural frequency response of the Chulitna River Bridge. These test results provide a baseline for the bridge condition in August 2012. In this report, we refer to the resulting experimental test data obtained from the “ambient” tests as *global* test data.

Local test data: On September 10, 2012, we load tested the Chulitna River Bridge with three loaded dump trucks. Seventeen different combinations of these trucks were used to statically and dynamically load test the bridge. The structural health monitoring system (SHMS)

was calibrated on September 9, 2012, in preparation for monitoring the structural response to these loaded trucks. Using SHMS, 73 sensors were monitored during testing. The sensor information (strains, temperatures, tilt displacements, and accelerations) are referred to as *local* experimental data.

Phase 1 – Ambient Tests (August 2012)

Short-term dynamic field vibrational tests were conducted on the Chulitna River Bridge in August 2012. An ambient free-decay response approach was used to estimate dynamic properties of the bridge. Stationary and dynamic tests were used to measure the acceleration response of the bridge at different locations and in different orientations during excitation caused by pedestrian traffic and ADOT&PF boom trucks. Natural frequencies were identified and characterized by fast Fourier transform (FFT) methods. The bridge's first eight tested modes are 1.50, 2.20, 2.85, 3.23, and 4.58 Hz. Of these tested modes, 2.85, 3.23, and 4.58 Hz are vertical modes and 1.50 and 2.20 Hz are longitudinal modes; the remaining three are transverse modes.

Fifteen portable single-axis accelerometers were used for the ambient tests (see Figs. E.1 and E.2). The accelerometers were located at piers and mid-spans. Because Spans 2, 3, and 4 are longer, more data collection points were placed in these spans. All accelerometers were set in a line along the center width of the deck on the flat clean driving surface. Vertical, transverse, and longitudinal accelerations were measured. In each, data were collected three times. Testing details are provided elsewhere (Xiao et al. 2012; Hulsey et al. 2012b; Hulsey et al. 2013a, 2013b; Xiao et al. 2014).

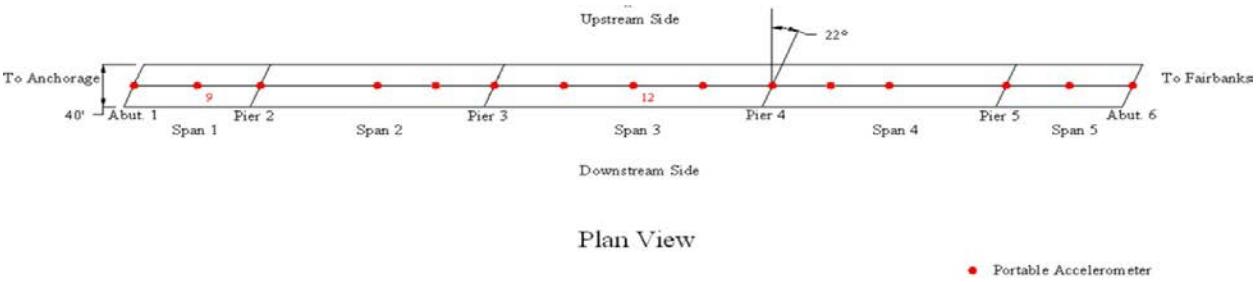

Figure E.1 Portable accelerometer location and number

Figure E.2 Application showing portable accelerometers

As part of the controlled ambient test, an A-30 ADOT&PF boom truck was used to excite the bridge. Traffic control was used to stop pedestrian traffic in an effort to isolate the excitation caused by the test vehicle. The bridge was closed to traffic and conditions were non-windy during the dynamic test. Every effort was made to reduce the influence of erroneous

input. The A-30 boom truck crossed the bridge from Fairbanks to Anchorage (traveling south) in the upstream lane at a speed of 45 mph (Fig. E.3). The bridge was kept closed while the bridge's excitation was monitored until vibration was totally damped out.

Figure E.3 A-30 boom truck traveling north for the dynamic ambient test

During the study, the research team found that recorded modal parameters are sensitive to sensor locations. Some locations are sensitive; some are not. At some locations, the output is too small to offer specific modal information reliably, or the information is too weak to be identified. As such, optimization was needed. In practice, multiple point measurements are needed to guarantee reliability and robustness of the measurement.

In the following figures and tables, we chose the two most sensitive data locations for processing. Figure E.4 shows the FFT of a typical measured acceleration signal in the vertical

direction in the middle of Span 3 (Point 12). In Figure E.4, we can see multiple peaks, with f_1=1.50 Hz, f_2=2.85 Hz, and f_3=3.23 Hz dominating.

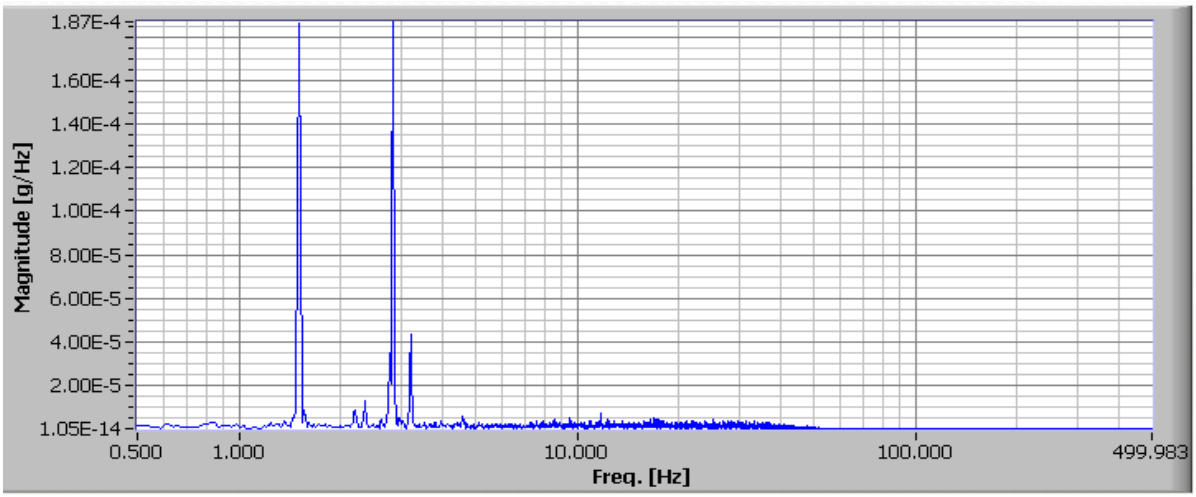

Figure E.4 FFT for measured vertical acceleration (middle of Span 3; Point 12)

Figure E.5 shows the FFT of a typical measured acceleration signal in the vertical direction in the middle of Span 1 (Point 9). In Figure E.5, we see multiple peaks, with f_{1a}=1.50 Hz, f_{2a}=2.20 Hz, f_{3a}=2.85 Hz, and f_{4a}=4.58 Hz dominating.

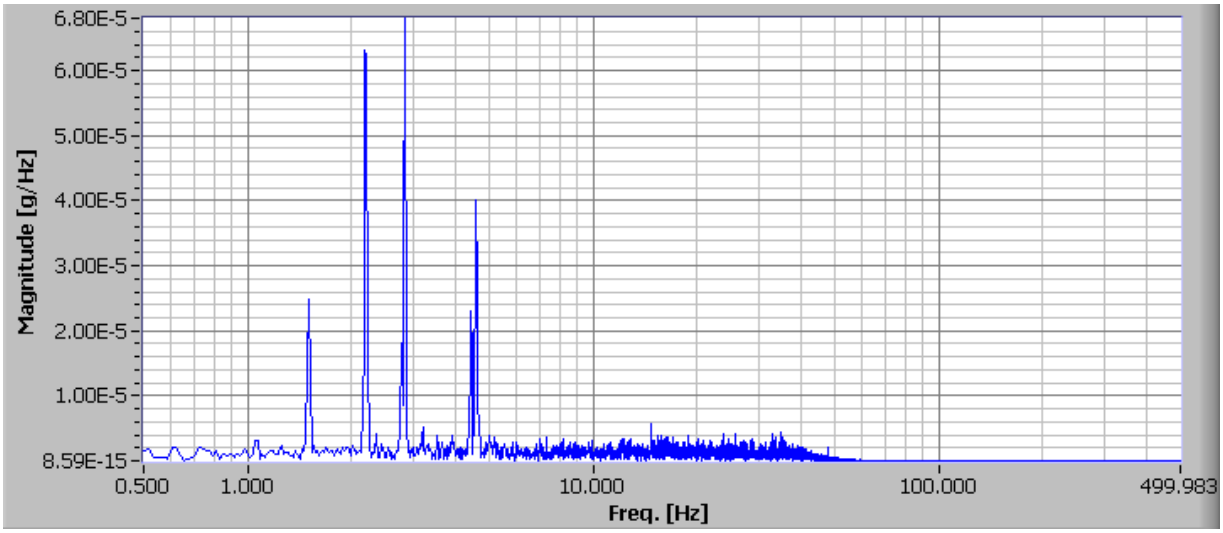

Figure E.5 FFT for measured vertical acceleration (middle of Span 1, Point 9)

Phase 1 – SHMS: Description of ADOT&PF Dump Truck Loading

Three ADOT&PF dump trucks were used to load test the Chulitna River Bridge on September 10, 2012. Prior to the load test, three empty ADOT&PF dump trucks were provided for testing the bridge. Each truck-trailer was weighed and measured. Then, the trailers were loaded with sand and the truck-trailers were weighed (this is the load prior to testing). At the end of the day on September 10, after the load test, the three loaded ADOT&PF dump trucks were again weighed. This data provided the researchers with a record of the change in weight over the 8-hour test period. Axle weights were measured with calibrated portable scales provided by the ADOT&PF (see Figs. E.6 and E.7).

Figure E.6 Axle weight measured by the wheel load scales

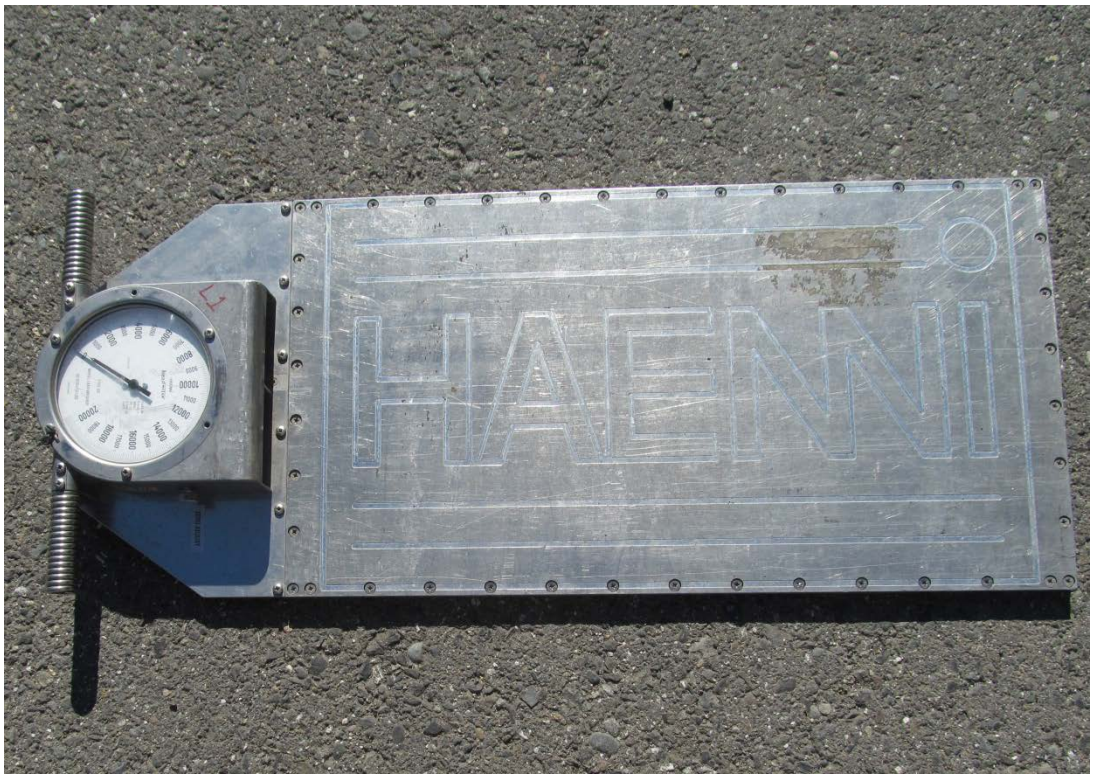

Figure E.7 Wheel load scales WL 101

Tables E.1 through E.3 are ADOT&PF dump truck measurement results from the portable weigh station. Load 1 was measured on September 9, the night before the load test, and Load 2 was measured on September 10, after the load test. Axle 1 is the steering axle (Fig. E.8).

Table E.1 Truck No. 36188 measurement results

	Measurement	Axle 1	Axle 2	Axle 3	Axle 4	Axle 5	Gross weight (lb)	Axle width
	Axle distance	15'3"	4'6"	29'1"	4'2"			
Truck 36188 (Heading) 37438 (Trailer)	Axle weight (Empty)	13,050 lb	8,100 lb	7,900 lb	4,800 lb	5,050 lb	38,900	6'6"
	Axle weight (Loaded 1)	13,200 lb	18,300 lb	18,400 lb	15,950 lb	16,250 lb	82,100	
	Axle weight (Loaded 2)	13,000 lb	18,400 lb	18,900 lb	16,650 lb	15,150 lb	82,100	

Table E.2 Truck No. 35752 measurement results

	Measurement	Axle 1	Axle 2	Axle 3	Axle 4	Axle 5	Gross weight (lb)	Axle width
Truck 35752 (Heading) 31526 (Trailer)	Axle distance	15'4"	4'5"	29'9"	4'1"			
	Axle weight (Empty)	12,550 lb	9,400 lb	9,100 lb	5,900 lb	5,800 lb	42,750	6'6"
	Axle weight (Loaded 1)	12,100 lb	18,850 lb	18,500 lb	15,500 lb	15,650 lb	80,600	
	Axle weight (Loaded 2)	12,300 lb	18,850 lb	18,850 lb	14,800 lb	15,550 lb	80,350	

Table E.3 Truck No. 36195 measurement results

	Measurement	Axle 1	Axle 2	Axle 3	Axle 4	Axle 5	Gross weight (lb)	Axle width
Truck 36195 (Heading) 36580 (Trailer)	Axle distance	16'9"	4'8"	28'9"	4'1"			
	Axle weight (Empty)	13,150 lb	7,950 lb	7,900 lb	3,200 lb	6,000 lb	38,200	6'8"
	Axle weight (Loaded 1)	13,350 lb	18,400 lb	18,100 lb	13,750 lb	16,650 lb	80,250	
	Axle weight (Loaded 2)	13,350 lb	18,450 lb	18,300 lb	12,150 lb	18,100 lb	80,350	

Figure E.8 Axle location

Phase 1 – Load Testing With Trucks

Heavily Loaded Trucks Load Test Trial 1 (Static)

In this test, two trucks were positioned with the trucks side-by-side (parallel) to the 22 angle (Fig. E.9) southbound at 1 mph. At each pier and at mid-span, the trucks were stopped for 30 seconds to record static response data. Truck No. 36188 was on the downstream side of the

bridge and Truck No. 36195 was on the upstream side of the bridge (see Tables E.1 through E.3 for truck weight, axle width, and axle spacing.

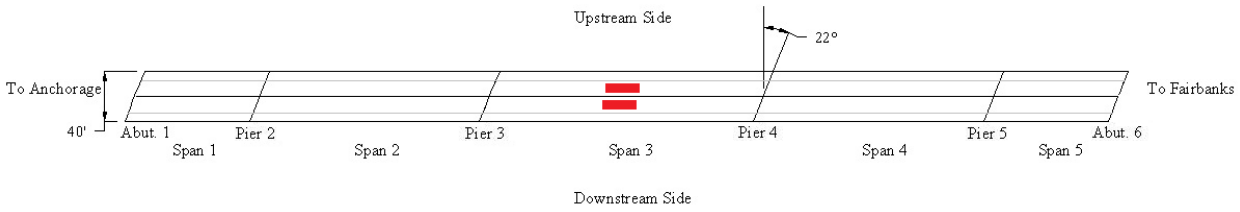

Figure E.9 Two trucks side-by-side and positioned in Span 3

In Trial 1, the ADOT&PF trucks used for testing were stopped and positioned in the middle of Span 3 (between Piers 3 and 4). The front axles were located 369 feet from the south abutment (Abutment 1) (see Figs. E.10 and E.11). A finite element analysis for these same load conditions was conducted. The local calculated strains and displacements were compared with the experimental SHMS response data

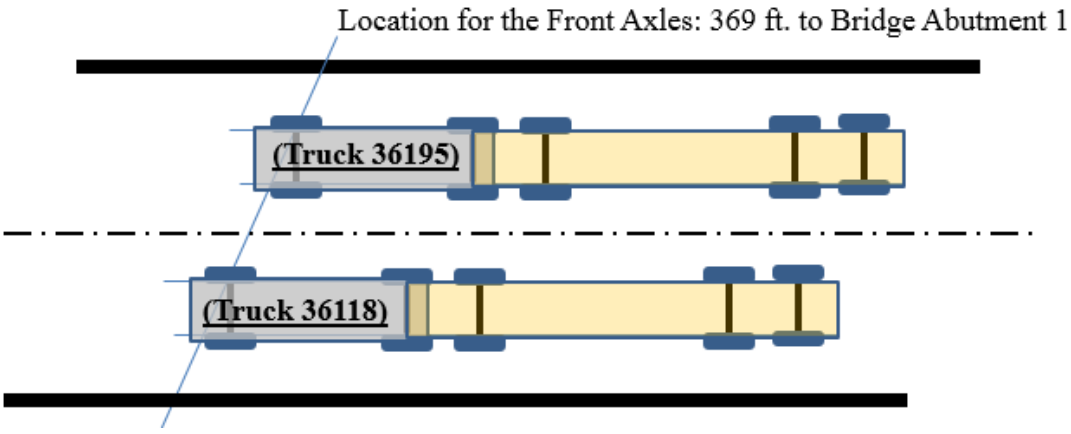

Figure E.10 Plan view of two trucks at mid-Span 3 southbound

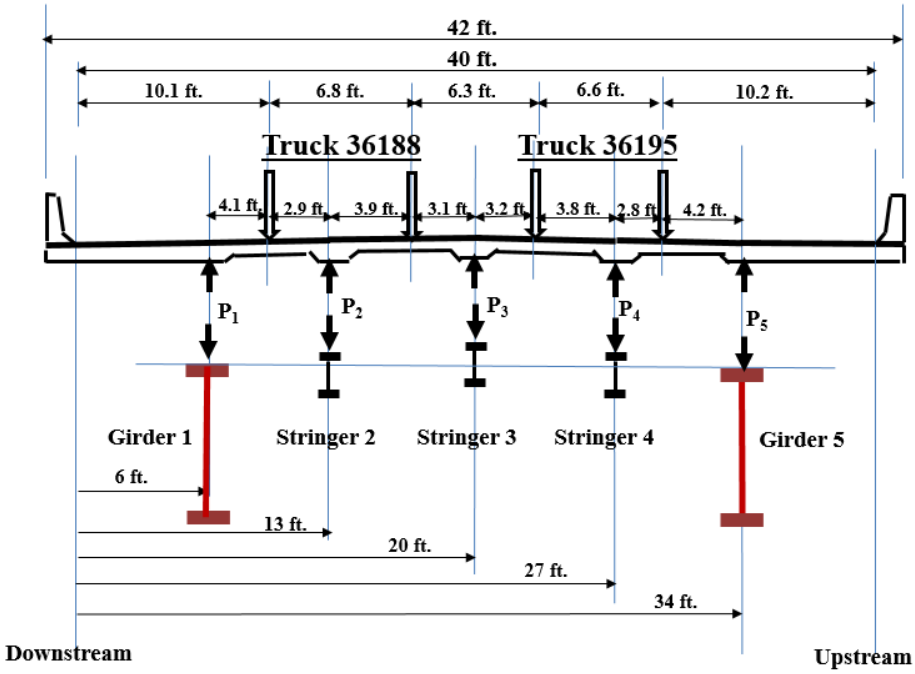

Figure E.11 Cross-sectional elevation view of two trucks at mid-Span 3

Heavily Loaded Trucks Load Test Trial 17 (Static)

Three trucks traveled parallel to the 22 degree skew angle of the bridge. Truck No. 36195 was on the upstream side of the bridge (Fig. E.12). The ADOT&PF loaded trucks moved southbound at 1 mph. We conducted static tests by stopping the trucks for no less than 30 seconds at several pre-determined locations along the length of the bridge. In Trial 17, three trucks were positioned at mid-span of Span 3 (see Figs. E.13 and E.14). We compared FEM calculated values with local SHMS data. Truck No. 36188 was on the middle of the bridge, and Truck No. 35752 was on the downstream side of the bridge (see Figs. E.13 and E.14).

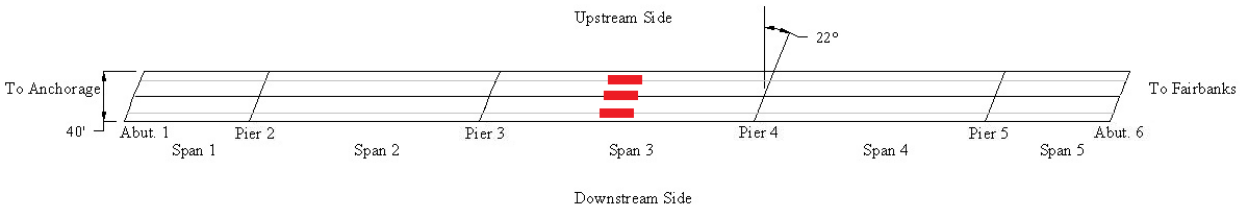

Figure E.12 Three trucks side by side

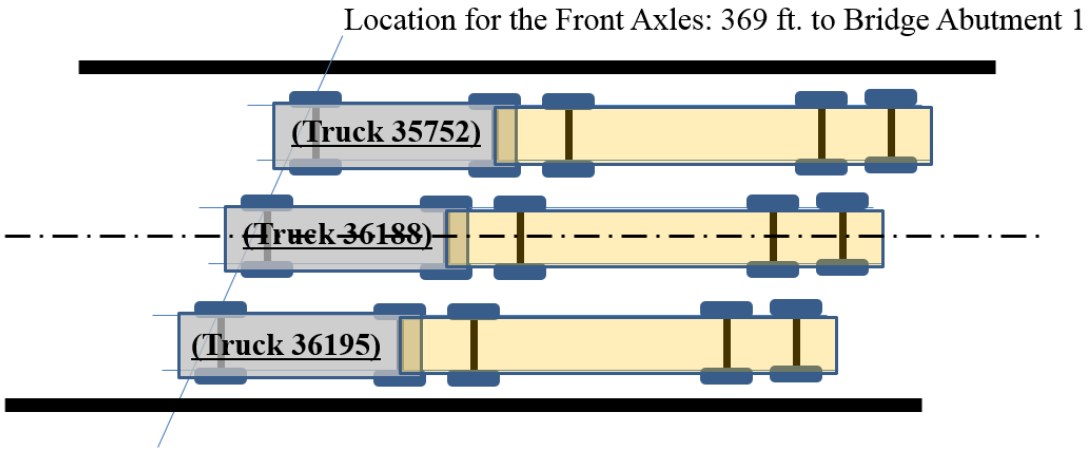

Figure E.13 Plan view of three trucks at mid-span southbound

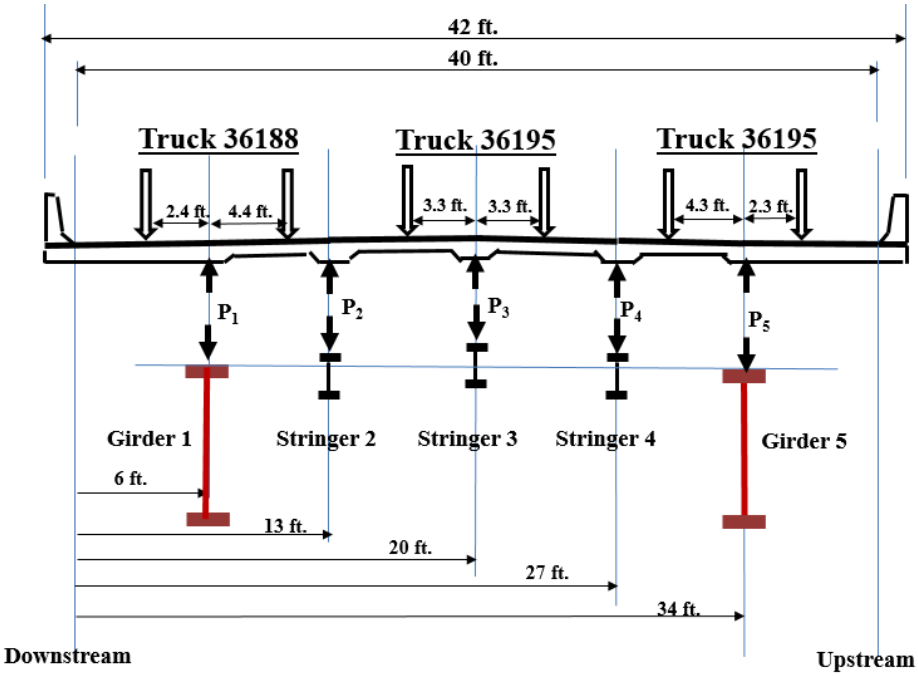

Figure E.14 Vertical view of three trucks at mid-span

Heavily Loaded Trucks Load Test Trial 6 (Dynamic)

In this test, the three ADOT&PF test trucks traveled side by side (Fig. E.15) heading north. Truck No. 36195 was in the downstream lane. Truck No. 36188 was in the middle lane and Truck No. 35752 was in the upstream lane. We requested that they travel as fast as they could safely cross the bridge. The ADOT&PF truck drivers selected a speed of 15 mph for this series of dynamic tests (see Fig. E.15 and Table E.4).

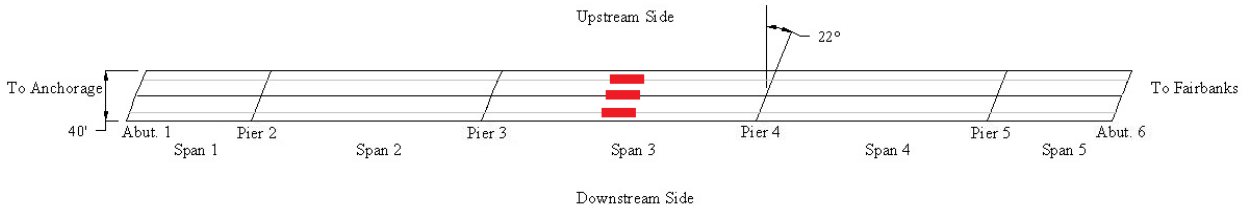

Figure E.15 Three trucks side by side

Table E.4 Dynamic load test Trial 6

Test	Type	Direction	Description	Time
6	Dynamic	North	Start Test	10:51
			End Test	10:53

Phase 2 – Ambient Tests (May 2013)

The ambient type of test is inexpensive and quick and can be done while performing a routine bridge inspection. The idea is to conduct this test to determine if the bridge may have undergone a significant change that is not visible to the naked eye. This tool does not provide the necessary information to identify a localized crack. It will provide an overall global evaluation in which a stiffness change has occurred. If a sufficient number of higher modes are monitored, it may be plausible to identify some localized issues. Additional research to evaluate the benefit of some of these issues is needed.

In May 2013, we conducted a second “ambient” test on the bridge; the first test was in August 2012. Again, we placed fifteen portable accelerometers in a line along the length of the bridge and located down the center of the driving surface (see Fig. E.16).

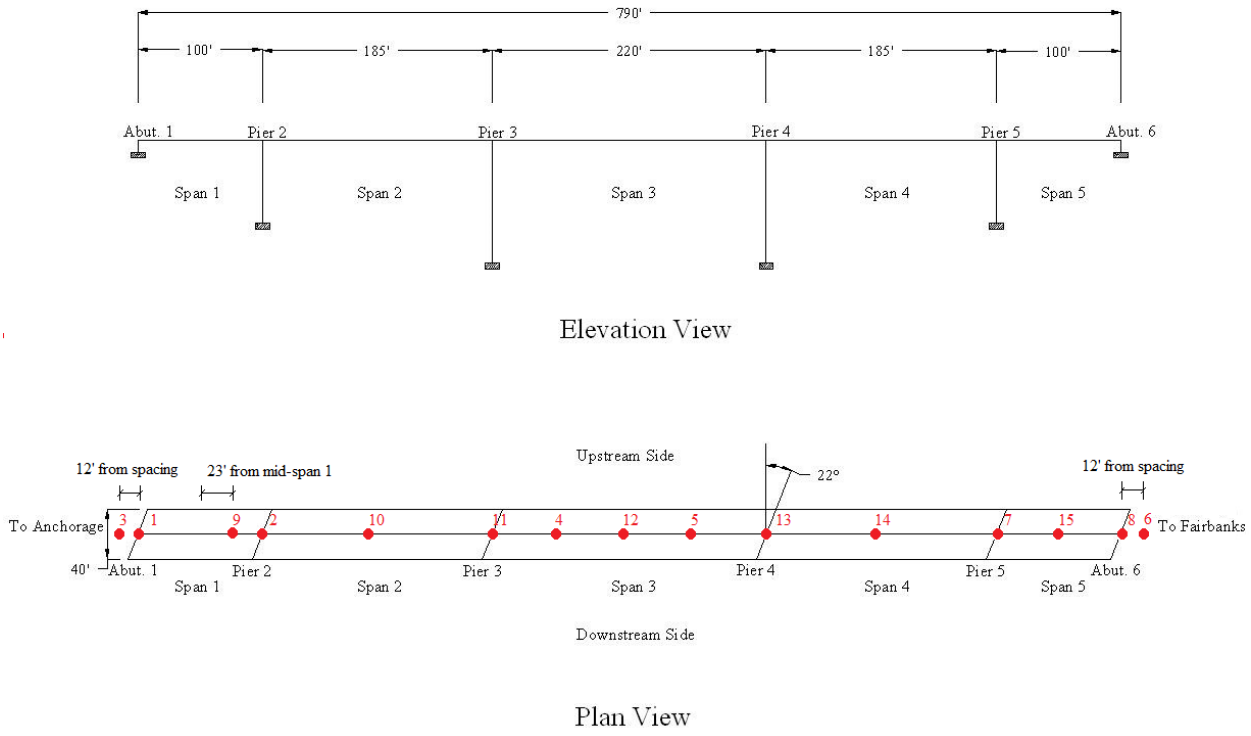

Figure E.16 Accelerometer layout

At the request of the research team, two test trials were performed. For Trial 1, ADOT&PF was asked to drive the boom truck across the bridge at 45 mph; this was done from north to south. Traffic was kept off the bridge while the acceleration data were recorded. This test was followed by Trial 2. In this case, ADOT&PF drove the boom truck from south to north. We repeated the testing procedure, in that traffic was stopped until we recorded the acceleration data. Table E.5 provides a summary of the difference between the 2012 and 2013 natural frequency data for the longitudinal and vertical modes. Table E.5 shows very little difference between natural frequencies in 2012 versus 2013. This result illustrates that there was effectively no

structural change in the behavior of the Chulitna River Bridge between 2012 and 2013. Table E.6 shows a correlation between the 2013 experimental data and the FEM calculated values.

Table E.5 The natural frequencies difference between 2012 and 2013

	2012 Ambient Test (Hz)	2013 Ambient Test (Hz)	100*[(Old-New)/Old]
Longitudinal Mode 1	1.500	1.500	0.000
Longitudinal Mode 2	2.190	2.206	-0.731
Vertical Mode 1	2.846	2.883	-1.300
Vertical Mode 2	3.224	3.236	-0.372
Vertical Mode 3	4.586	4.617	-0.676

Table E.6 Natural frequencies difference between 2013 field measurement and updated model

Mode	Field Measurement (Hz)	FEM Results (Hz)	Difference (%)
Longitudinal Mode 1	1.500	1.367	8.9
Longitudinal Mode 2	2.206	2.044	7.3
Vertical Mode 1	2.883	2.756	4.4
Vertical Mode 2	3.236	3.348	-3.46
Vertical Mode 3	4.617	4.249	8.0